JACS
JOURNAL OF THE AMERICAN CHEMICAL SOCIETY
pubs.acs.org/JACS
Communication

Visible Light-Induced Specific Protein Reaction Delineates Early Stages of Cell Adhesion

Rolle Rahikainen, Susan K. Vester, Paula Turkki, Chasity P. Janosko, Alexander Deiters, Vesa P. Hytönen,* and Mark Howarth*

Cite This: https://doi.org/10.1021/jacs.3c07827
Read Online

ABSTRACT: Light is well-established for control of bond breakage but not for control of specific bond formation in complex environments. We previously engineered the diffusion-limited reactivity of the SpyTag003 peptide with its protein partner SpyCatcher003 through spontaneous isopeptide bond formation. This system enables precise and irreversible assembly of biological building blocks with applications from biomaterials to vaccines. Here we establish a system for the rapid control of this amide bond formation with visible light. We have generated a caged SpyCatcher003, which allows light triggering of covalent bond formation to SpyTag003 in mammalian cells. Photocaging is achieved through site-specific incorporation of an unnatural coumarin-lysine at the reactive site of SpyCatcher003. We showed a uniform specific reaction in cell lysate upon light activation. We then used the spatiotemporal precision of a 405 nm confocal laser for uncaging in seconds, probing the earliest events in mechanotransduction by talin, the key force sensor between the cytoskeleton and the extracellular matrix. Reconstituting talin induced rapid biphasic extension of lamellipodia, revealing the kinetics of talin-regulated cell spreading and polarization. Thereafter we determined the hierarchy of the recruitment of key components for cell adhesion. Precise control over site-specific protein reaction with visible light creates diverse opportunities for cell biology and nanoassembly.

Living systems display exquisite precision in their organization and rapid adaptation. Chemical biology aims to exert control over cell or organism behavior, but most methods act over hours to days (genetic modification) or lack spatial control (pharmacological manipulation).[1,2] However, light allows rapid and precise subcellular responses, e.g., optogenetics to modulate membrane gradients for electrical signaling.[3] In the area of protein interactions, interactions can be switched by visible light using phytochrome or light-oxygen voltage (LOV) domains.[1] We have endeavored to develop protein−protein interactions that extend beyond typical stability through genetically encoded irreversible ligation.[4] SpyTag003 is a peptide that we engineered for rapid isopeptide bond formation with its protein partner SpyCatcher003 (Figure 1A).[5] Reaction proceeds close to the diffusion limit, occurs under diverse conditions, and is efficient in numerous cellular systems.[5,6] Tag/Catcher bioconjugation has been employed in biomaterials, vaccine assembly, and antibody functionalization.[4,7−9] SpyTag003/SpyCatcher003 has also been useful inside cells, including recruitment of epigenetic modifiers or enzyme channeling.[4,10,11] Previously, an engineered LOV domain allowed photocontrol of SpyTag/SpyCatcher, although there was gradual isopeptide bond formation even in the dark state.[12] To enable highly switchable covalent reaction, here we employ site-specific incorporation of an unnatural amino acid.[13] Photoreactive amino acids like benzoylphenylalanine trap complexes after UV activation,[14] which is powerful to identify unknown complexes but not ideal for targeted bridging.[14] Individual amino acids can also be photocaged,[13,15,16] and K31 is the key reactive residue on SpyCatcher003 (Figure 1A).[5] We focused our efforts on the unnatural amino acid 7-hydroxycoumarin lysine (HCK) (Figure 1B) because uncaging in the visible spectrum (Figure 1C) would reduce phototoxicity that is particularly serious in the UV range.[15,17,18] Here we establish caging of SpyCatcher003 using unnatural coumarin-lysine amino acid and its uncaging with 405 nm light for spatiotemporal control in living cells to reveal early steps in mammalian cell adhesion.

To establish our uncaging approach, we cotransfected the human cell-line HEK293T with HCK tRNAs and HCK tRNA synthetase (HCK RS)[19,20] along with our protein of interest to show that expression depended on the unnatural amino acid. Our initial construct contained the N-terminal region of transferrin receptor (TfR), SpyCatcher003 with an amber stop codon at K31 (K31TAG), and superfolder green fluorescent protein (sfGFP). Based on Western blotting, we optimized the dose of HCK and the ratio of the SpyCatcher003 construct to HCK RS (Figure S1A).

We then applied a photocontrolled reaction to gain insight into cell adhesion, focusing on talin protein. Talin bridges the cytoplasmic domain of β-integrin to the actin cytoskeleton and functions as a molecular clutch required for actin-dependent cell spreading.[21−23] Talin changes conformation in response to force, regulating association and release of multiple proteins

Received: July 21, 2023
Revised: October 24, 2023
Accepted: October 25, 2023

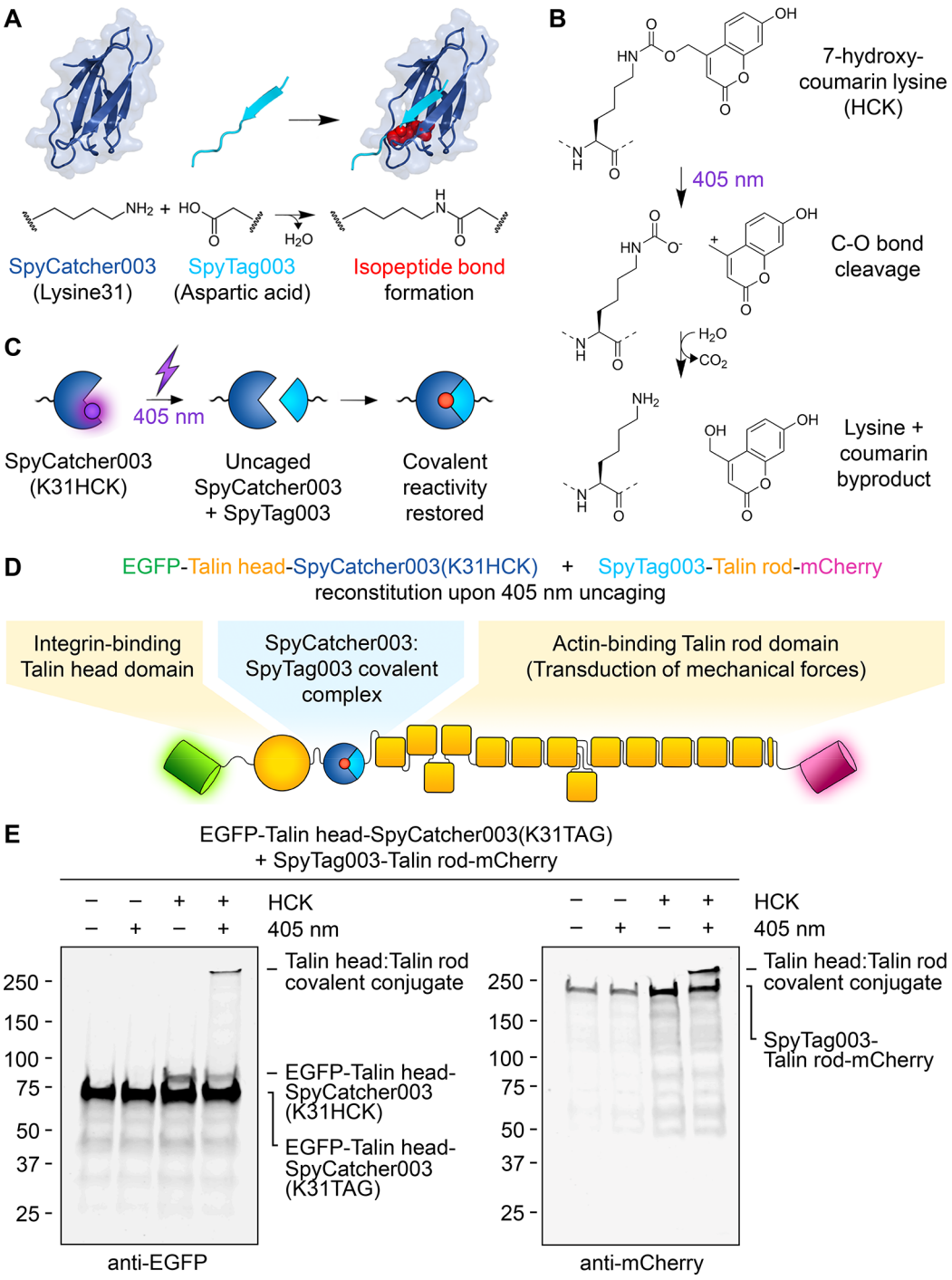

Figure 1. SpyCatcher003 photocaging with 7-hydroxycoumarin lysine. (A) Schematic of the SpyTag003/SpyCatcher003 reaction. Lysine on SpyCatcher003 (dark blue) and aspartic acid on SpyTag003 (cyan) form a spontaneous isopeptide bond (reacted side chains shown as red spheres), based on PDB entry 4MLI. (B) Schematic of the light-induced cleavage. Dotted lines indicate the rest of the polypeptide. (C) Schematic for SpyCatcher003(K31HCK) uncaging. (D) Split talin reconstitution using SpyCatcher003(K31HCK). (E) Covalent talin reconstitution upon SpyCatcher003(K31HCK) photoactivation. Talin knockout cells transfected with EGFP-Talin head-SpyCatcher003(K31HCK) and SpyTag003-Talin rod-mCherry were analyzed ± HCK and ± 405 nm light, before Western blotting with anti-EGFP (left) or anti-mCherry (right).

involved in the cell's response to mechanical cues.[24] Talin recruitment has been previously controlled by an elegant strategy using rapamycin as a cell-permeable small molecule to reconstitute FRB- and FKBP-split talin fragments.[25] However, this approach lacks subcellular spatial resolution and was only tested to withstand force of 4 pN,[25] which may not resist sustained cytoskeletal tension acting on talin at 10−40 pN.[26,27] Split talin reconstitution using LOV domains would allow spatial control but depends on continuous 488 nm illumination and has limited interaction stability.[28] Because of the complex structure and natural turnover of adhesion structures, estimating the impact of such non-covalently reconstituted talin on adhesion function is challenging. Rapid light-mediated induction of covalent talin reconstitution would allow precise control over early phases of adhesion formation to decipher molecular details of talin-dependent processes.

https://doi.org/10.1021/jacs.3c07827
J. Am. Chem. Soc. XXXX, XXX, XXX−XXX

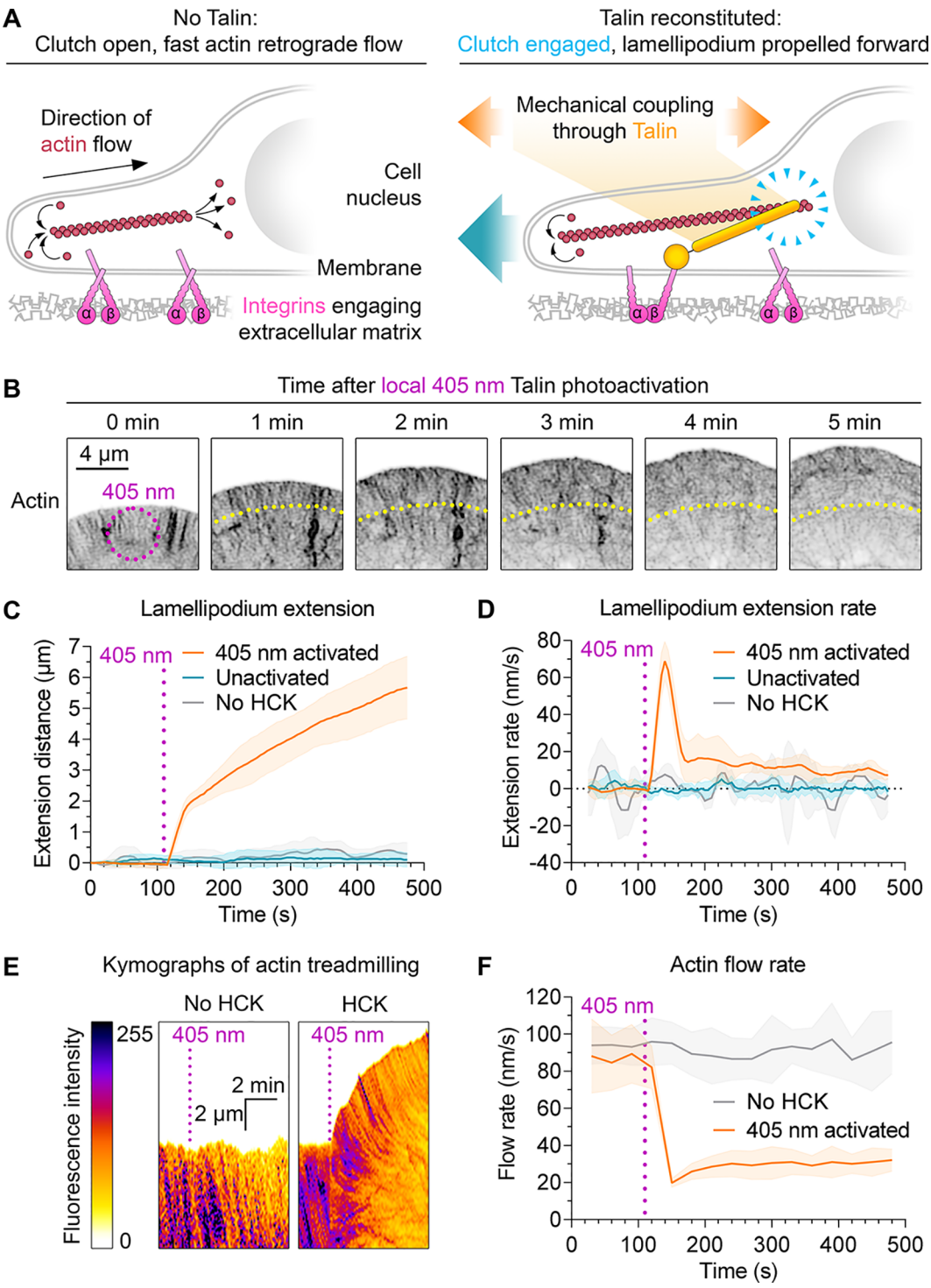

Figure 2. Photocontrol of SpyTag003/SpyCatcher003 reactivity in living cells. (A) Schematic of talin's role as an adhesion clutch. (B) Photoactivation of cell spreading. Talin knockout cells transfected with caged split talin were activated by 405 nm light for 5 s (magenta ring) and imaged at the indicated time points. Inverted LifeAct-mNeonGreen signal for actin is shown. Yellow indicates the original lamellipodium edge. (C, D) Quantification of the lamellipodium extension distance and extension rate. Cells were activated as in (B) and imaged for LifeAct-mNeonGreen. $n = 5-11$ cells. (E) Actin dynamics after photoactivation. Cells were activated as in (B), and kymographs were created for lamellipodium LifeAct-mNeonGreen. (F) Quantification of actin treadmilling. Magenta indicates the point of 405 nm activation. Line represents mean, with shading ±1 SD, $n = 6-8$ cells.

To establish optical control of talin reconstitution, we incorporated SpyCatcher003(K31TAG) in a split talin construct (Figure 1D). We studied HCK- and light-dependent covalent talin reconstitution in fibroblast cells by Western blot against EGFP or mCherry. HCK-caged SpyCatcher003 did not react with SpyTag003 until cells were treated with 405 nm light, consistent with the effective caging of SpyCatcher003 (Figure 1E). We confirmed this tight control of SpyCatcher reactivity also in a different setup, using recombinant SpyTag003-maltose-binding protein (MBP) to probe for SpyCatcher003(K31HCK)

https://doi.org/10.1021/jacs.3c07827
J. Am. Chem. Soc. XXXX, XXX, XXX−XXX

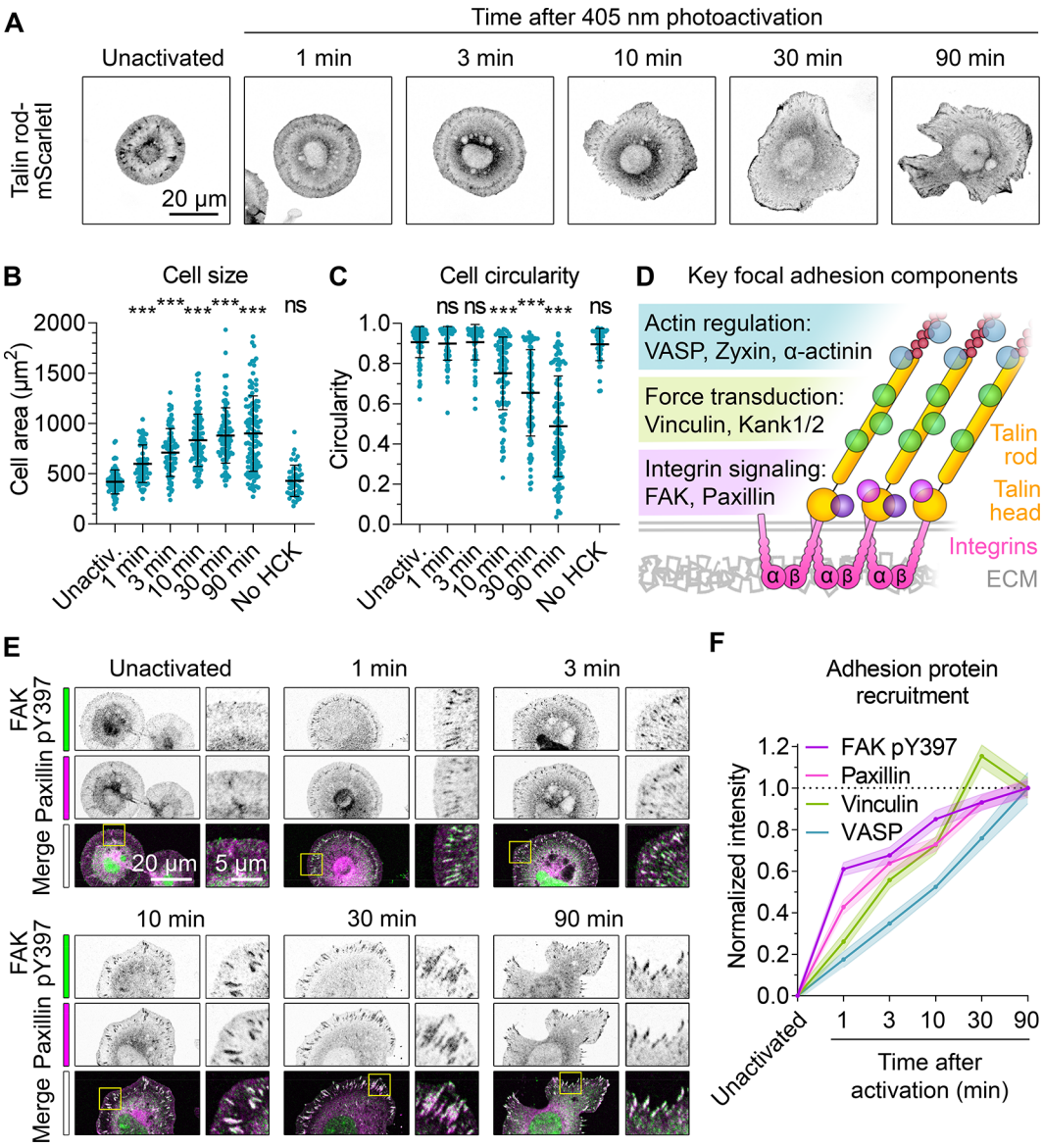

Figure 3. Photoactivation of talin allows precise control over adhesion complex formation, cell spreading, and polarization. (A) Cell spreading and polarization after photoactivation. Talin knockout cells expressing Talin head-SpyTag003, SpyCatcher003(K31HCK)-Talin rod-mScarletI, HCK tRNAs, and HCK RS were activated by 405 nm wide-field illumination for 1 min and fixed at the indicated time, before fluorescence microscopy for mScarletI. (B, C) Quantification of cell size and circularity following talin photoactivation as in (A). Each blue circle is one cell, with black lines showing mean ± 1 SD. Compared with unactivated cells using one-way ANOVA and Dunnett's test: *** $p < 0.0001$, ns $p > 0.05$, $n = 45–110$ cells from two independent experiments. (D) Schematic of key adhesion components. Interactions with talin's rod domain generate three functional layers (colored bars). (E) Recruitment of adhesion components after talin photoactivation. Talin knockout cells were photoactivated as in (A) and stained with antibodies for fluorescence microscopy (zoom of the yellow square in the right image). Overlap of FAK pY397 (green) and paxillin (magenta) in the merge shows as white. (F) Quantification of recruitment to adhesions following talin photoactivation as in (E). Line represents the mean, with shading ±1 SEM, $n = 60–85$ adhesions in 12−17 cells from two independent experiments.

reactivity in cell lysates (Figure S1B,C). Western blot with antiserum to SpyCatcher003 (Figure S1B) or anti-EGFP (Figure S1C) demonstrated light-dependent SpyCatcher003-(K31HCK) activation and isopeptide bond formation. Without HCK, no SpyCatcher003 expression was detected, indicating that the stop codon led to chain termination (Figure S1B). To understand the practicality for selective uncaging, we assessed uncaging by ambient light. Room lighting or U.K. sunlight for 120 min did not lead to substantial uncaging in cell lysate in microcentrifuge tubes (Figure S2). Depending on the used wavelength and required light dose, optogenetic control of cells even with visible light can lead to phototoxicity.[29] We confirmed the biocompatibility of 405 nm light on fibroblast cells using a resazurin-based metabolic activity assay. We observed full viability of cells in Trolox-supplemented media even after 3 min of continuous 405 nm exposure (Figure S3).

Having confirmed robust 405 nm photouncaging, we investigated the effects of talin reconstitution in fibroblasts with knockout of both endogenous talin genes.[21] We transfected with Talin head-SpyTag003 and SpyCatcher003(K31HCK)-Talin rod-mScarletI, along with HCK tRNAs and HCK RS with LifeAct-mNeonGreen to visualize actin. Cells were cultured with HCK and imaged by confocal microscopy with lasers at 405 nm (photoactivation), 488 nm (mNeonGreen, a bright-green

https://doi.org/10.1021/jacs.3c07827
J. Am. Chem. Soc. XXXX, XXX, XXX−XXX

fluorescent protein), and 561 nm (mScarletI, a bright-red fluorescent protein). Unactivated cells could not spread or polarize, consistent with the lack of functional talin (Figure 2A).[21,23] Local photoactivation at 405 nm for 5 s led to lamellipodia extension within seconds (Figure 2B,C and Movie S1), indicating the rapid reconstitution of talin in cells. We did not observe spreading of unactivated cells imaged at 488 nm (Figure 2C and Movie S1), so typical microscopy conditions did not cause unintended photoactivation. Similarly, we did not observe spreading upon 405 nm exposure of cells transfected as described above but with the equivalent DMSO concentration in place of HCK (Figure 2C).

Upon talin reconstitution, we observed biphasic extension of lamellipodia, with a fast initial phase (∼70 nm/s) followed by a slower phase (10−20 nm/s) (Figure 2C,D). Actin polymerization at the cell periphery is the main driving force propelling the lamellipodium forward,[30] so we investigated actin treadmilling by tracking LifeAct-mNeonGreen (Figure 2E). Unactivated cells had a fast initial actin rearward flow at ∼90 nm/s (Figure 2F). Talin reconstitution led to a sharp drop to ∼20 nm/s, followed by a gradual recovery to ∼30 nm/s (Figure 2F). The sharp drop in actin retrograde flow coincides with the phase of fast lamellipodium extension, suggesting that the integrin−talin−actin clutch is rapidly engaged upon talin photoactivation.

Force sensing by talin generates localized activation of adhesion signaling, regulating cell polarization.[23] Given the covalent SpyTag003:SpyCatcher003 interaction, this photoactivation strategy should allow extended cell polarization experiments covering tens of minutes. Talin knockout fibroblasts transfected with Talin head-SpyTag003, SpyCatcher003(K31HCK)-Talin rod-mScarletI, and HCK RS plasmids were cultured with HCK and photoactivated with wide-field 405 nm light for 1 min. Cells were fixed at selected time points and analyzed for cell area and morphology. Activated cells showed fast initial spreading and reached close to a maximal area ∼10 min after photoactivation (Figure 3A,B). In contrast, cell polarization was triggered only when the maximal cell area was reached and continued to develop until the end of the experiment (Figure 3C). As expected, cells without HCK did not react to the photoactivation stimulus (Figure 3B,C).

We next explored the feasibility of fine-tuning SpyTag003/SpyCatcher003 light regulation via single or double amino acid mutations in SpyTag003 (Figure S4A).[5] We observed reduced spreading of unactivated cells expressing SpyTag003 mutants compared to SpyTag003 itself (Figure S4B,C), suggesting that SpyCatcher003(K31HCK) may form a transient non-covalent complex with SpyTag003 before uncaging. While the SpyTag003(V114T, V116T) complex was unable to mediate stable talin reconstitution and adhesion formation in the absence of light, cell spreading and polarization were equivalent to SpyTag003 after 405 nm activation (Figure S4B,C). SpyTag003(M115G) did allow increased cell spreading after light activation but showed little cell polarization (Figure S4B-D). Therefore, these peptide variants provide alternative properties for light-regulated peptide−protein interaction.

Stretching of talin rod regulates recruitment and release of many adhesion components, generating a structure with distinct functional layers (Figure 3D).[31] However, the heterogeneous and dynamic structure of adhesion complexes makes it challenging to define the temporal hierarchy of adhesion protein recruitment.[32] Having validated our method for triggering synchronized adhesion, we investigated the rates of recruitment for key adhesion components. Focal adhesion kinase (FAK) is a central adhesion complex tyrosine kinase that is activated by phosphorylation at tyrosine 397 (pY397).[33] Paxillin is an adaptor protein interacting with both structural and signaling components.[33] Vinculin is recruited to mechanically activated sites in the talin rod domain and binds F-actin to reinforce mechanically the adhesion complex.[23,34] Vasodilator-stimulated phosphoprotein (VASP) is an actin regulator, promoting actin filament elongation through multiple mechanisms.[30] We observed fast initial FAK pY397 recruitment to adhesions, reaching half-maximal intensity <1 min after photoactivation (Figures 3E,F and S5B). Paxillin and vinculin reached half-maximal intensity at 3 min, with paxillin being slightly faster (Figures 3E,F and S5A,C,D). In contrast, recruitment of VASP reached half-maximal intensity only after 10 min (Figures 3F and S5A,E).

Robust optical control of protein complexation relies on a sufficient bond life of the activated complex, ideally exceeding the natural turnover rate of the studied proteins. Interaction stability is especially challenging when the interface is under mechanical tension. Careful analysis of interface stability has allowed the use of elegant non-covalent optogenetic tools in reconstituting force-bearing proteins.[28,35] However, local changes in force magnitude, duration, and application rate can affect bond stability and lead to inconsistent or unrepresentative results. To overcome this limitation, we developed SpyCatcher003(K31HCK) for visible-light photoactivation and demonstrated its application in the covalent reconstitution of split talin. Optical control of talin reconstitution allowed us to probe the time scale of initial adhesion complex formation, revealing biphasic extension of lamellipodia upon engagement of the adhesion clutch. We also demonstrated the use of SpyCatcher003(K31HCK) coupling over a longer time course, establishing a hierarchy of adhesion protein recruitment after engaging the adhesion clutch. The recruitment rates of adhesion proteins followed the layer structure of the adhesion complex (Figure 3D),[31,32] suggesting that talin governs not only the nanoscale organization of the adhesion but also the timing of protein recruitment.

Light control of covalent reactivity can also be achieved with bispecific molecules regulating the bridging of SNAP-tag (19 kDa) with HaloTag (33 kDa).[36,37] However, the larger size of this protein pair may reduce the range of accessible sites. Split intein reaction may also be regulated by photocaged tyrosine, but the reconstitution over 4 h may limit applicability for cellular processes.[38] While this work was in progress, a related approach was reported with photocaging of the slower first-generation SpyCatcher using *o*-nitrobenzyloxycarbonyl-caged lysine.[39] This approach used 365 nm wide-field uncaging with a 20 min uncaging time. Hence, the 405 nm-responsive amino acid used here should have lower phototoxicity for cell biology studies.[17,40−42] Also, 405 nm lasers are common on confocal microscopes, allowing uncaging at a spatiotemporal resolution not easily achieved by using 365 nm wide-field light sources and photomasks.

Beyond adhesion, SpyCatcher003(K31HCK) may become a broadly applicable tool for the photocontrol of biomolecules. A robust cellular response was initiated in seconds here, opening possibilities for spatiotemporal control of highly dynamic intracellular and extracellular processes.

https://doi.org/10.1021/jacs.3c07827
J. Am. Chem. Soc. XXXX, XXX, XXX−XXX

■ ASSOCIATED CONTENT

Supporting Information

The Supporting Information is available free of charge at https://pubs.acs.org/doi/10.1021/jacs.3c07827.

Western blots for the validation of SpyCatcher003-(K31HCK) photoactivation (Figure S1); Western blot to validate stability of SpyCatcher003(K31HCK) in ambient light (Figure S2); phototoxicity assay for 405 nm exposure on fibroblast cells (Figure S3); cell morphology analysis for cells expressing mutated SpyTag variants (Figure S4); representative images of vinculin and VASP recruitment and raw data for adhesion protein recruitment analysis (Figure S5); methods section (PDF)

Time-lapse image series of cell spreading upon 405 nm photoactivation of talin reconstitution (Movie S1) (AVI)

■ AUTHOR INFORMATION

Corresponding Authors

Mark Howarth − *Department of Biochemistry, University of Oxford, Oxford OX1 3QU, U.K.; Department of Pharmacology, University of Cambridge, Cambridge CB2 1PD, U.K.;* orcid.org/0000-0001-8870-7147; Email: mh2186@cam.ac.uk

Vesa P. Hytönen − *Faculty of Medicine and Health Technology, Tampere University, 33520 Tampere, Finland; Fimlab Laboratories, 33520 Tampere, Finland;* orcid.org/0000-0002-9357-1480; Email: vesa.hytonen@tuni.fi

Authors

Rolle Rahikainen − *Faculty of Medicine and Health Technology, Tampere University, 33520 Tampere, Finland; Fimlab Laboratories, 33520 Tampere, Finland;* orcid.org/0000-0003-1265-862X

Susan K. Vester − *Department of Biochemistry, University of Oxford, Oxford OX1 3QU, U.K.;* Present Address: Randall Centre for Cell and Molecular Biophysics, King's College London, New Hunt's House, London SE1 1UL, U.K; orcid.org/0000-0002-4210-118X

Paula Turkki − *Faculty of Medicine and Health Technology, Tampere University, 33520 Tampere, Finland; Fimlab Laboratories, 33520 Tampere, Finland*

Chasity P. Janosko − *Department of Chemistry, University of Pittsburgh, Pittsburgh, Pennsylvania 15260, United States*

Alexander Deiters − *Department of Chemistry, University of Pittsburgh, Pittsburgh, Pennsylvania 15260, United States;* orcid.org/0000-0003-0234-9209

Complete contact information is available at: https://pubs.acs.org/10.1021/jacs.3c07827

Notes

The authors declare the following competing financial interest(s): M.H. is an inventor on patents on spontaneous amide bond formation (EP2534484) and SpyTag003:SpyCatcher003 (U.K. Intellectual Property Office 1706430.4) and is a SpyBiotech co-founder and shareholder.

■ ACKNOWLEDGMENTS

Funding was provided by Biotechnology and Biological Sciences Research Council (BBSRC) (BB/T004983/1, S.K.V. and M.H.) and Academy of Finland postdoctoral researcher funding (339449, R.R.). We acknowledge Academy of Finland (331946, V.P.H.), Cancer Foundation Finland (V.P.H.), Sigrid Juselius Foundation (V.P.H.), and National Institutes of Health (R01AI175067, A.D.) for financial support. The authors acknowledge the Biocenter Finland and Tampere Imaging Facility for service and infrastructure support. We thank Prof. Reinhard Fässler (Max Planck Institute of Biochemistry) and Prof. Carsten Grashoff (University of Münster) for help with the talin knockout fibroblasts. For the purpose of Open Access, the author has applied a CC BY public copyright license to any Author Accepted Manuscript (AAM) version arising from this submission.

■ REFERENCES

(1) Seong, J.; Lin, M. Z. Optobiochemistry: Genetically Encoded Control of Protein Activity by Light. *Annu. Rev. Biochem.* **2021**, *90*, 475−501.

(2) Way, J. C.; Collins, J. J.; Keasling, J. D.; Silver, P. A. Integrating Biological Redesign: Where Synthetic Biology Came from and Where It Needs to Go. *Cell* **2014**, *157*, 151−161.

(3) Sittewelle, M.; Ferrandiz, N.; Fesenko, M.; Royle, S. J. Genetically Encoded Imaging Tools for Investigating Cell Dynamics at a Glance. *J. Cell Sci.* **2023**, *136* (7), No. jcs260783.

(4) Keeble, A. H.; Howarth, M. Power to the Protein: Enhancing and Combining Activities Using the Spy Toolbox. *Chem. Sci.* **2020**, *11*, 7281−7291.

(5) Keeble, A. H.; Turkki, P.; Stokes, S.; Khairil Anuar, I. N. A.; Rahikainen, R.; Hytönen, V. P.; Howarth, M. Approaching Infinite Affinity through Engineering of Peptide-Protein Interaction. *Proc. Natl. Acad. Sci. U.S.A.* **2019**, *116*, 26523−26533.

(6) Napierski, N. C.; Granger, K.; Langlais, P. R.; Moran, H. R.; Strom, J.; Touma, K.; Harris, S. P. A Novel "Cut and Paste" Method for In Situ Replacement of cMyBP-C Reveals a New Role for cMyBP-C in the Regulation of Contractile Oscillations. *Circ. Res.* **2020**, *126* (6), 737−749.

(7) Sun, F.; Zhang, W.-B.; Mahdavi, A.; Arnold, F. H.; Tirrell, D. A. Synthesis of Bioactive Protein Hydrogels by Genetically Encoded SpyTag-SpyCatcher Chemistry. *Proc. Natl. Acad. Sci. U.S.A.* **2014**, *111* (31), 11269−11274.

(8) Orozco-Hidalgo, M. T.; Charrier, M.; Tjahjono, N.; Tesoriero, R. F.; Li, D.; Molinari, S.; Ryan, K. R.; Ashby, P. D.; Rad, B.; Ajo-Franklin, C. M. Engineering High-Yield Biopolymer Secretion Creates an Extracellular Protein Matrix for Living Materials. *mSystems* **2021**, *6* (2), e00903−20.

(9) Zhang, F.; Zhang, W.-B. Encrypting Chemical Reactivity in Protein Sequences toward Information-Coded Reactions. *Chin. J. Chem.* **2020**, *38* (8), 864−878.

(10) Swain, T.; Pflueger, C.; Freytag, S.; Poppe, D.; Pflueger, J.; Nguyen, T.; Li, J. K.; Lister, R. A Modular dCas9-Based Recruitment Platform for Combinatorial Epigenome Editing. *bioRxiv* **2022**, DOI: 10.1101/2022.07.01.498378.

(11) Wei, Q.; He, S.; Qu, J.; Xia, J. Synthetic Multienzyme Complexes Assembled on Virus-like Particles for Cascade Biosynthesis In Cellulo. *Bioconjugate Chem.* **2020**, *31* (10), 2413−2420.

(12) Hartzell, E. J.; Terr, J.; Chen, W. Engineering a Blue Light Inducible SpyTag System (BLISS). *J. Am. Chem. Soc.* **2021**, *143* (23), 8572−8577.

(13) Chin, J. W. Expanding and Reprogramming the Genetic Code of Cells and Animals. *Annu. Rev. Biochem.* **2014**, *83*, 379−408.

(14) Fu, X.; Chang, Z. Biogenesis, Quality Control, and Structural Dynamics of Proteins as Explored in Living Cells via Site-Directed Photocrosslinking. *Protein Sci.* **2019**, *28* (7), 1194−1209.

(15) Baker, A. S.; Deiters, A. Optical Control of Protein Function through Unnatural Amino Acid Mutagenesis and Other Optogenetic Approaches. *ACS Chem. Biol.* **2014**, *9*, 1398−1407.

(16) Gautier, A.; Nguyen, D. P.; Lusic, H.; An, W.; Deiters, A.; Chin, J. W. Genetically Encoded Photocontrol of Protein Localization in Mammalian Cells. *J. Am. Chem. Soc.* **2010**, *132*, 4086−4088.

(17) Zhou, W.; Deiters, A. Chemogenetic and Optogenetic Control of Post-Translational Modifications through Genetic Code Expansion. *Curr. Opin. Chem. Biol.* **2021**, *63*, 123−131.
(18) Liu, J.; Hemphill, J.; Samanta, S.; Tsang, M.; Deiters, A. Genetic Code Expansion in Zebrafish Embryos and Its Application to Optical Control of Cell Signaling. *J. Am. Chem. Soc.* **2017**, *139* (27), 9100−9103.
(19) Luo, J.; Uprety, R.; Naro, Y.; Chou, C.; Nguyen, D. P.; Chin, J. W.; Deiters, A. Genetically Encoded Optochemical Probes for Simultaneous Fluorescence Reporting and Light Activation of Protein Function with Two-Photon Excitation. *J. Am. Chem. Soc.* **2014**, *136*, 15551−15558.
(20) Zhou, W.; Wesalo, J. S.; Liu, J.; Deiters, A. Genetic Code Expansion in Mammalian Cells: A Plasmid System Comparison. *Bioorg. Med. Chem.* **2020**, *28* (24), No. 115772.
(21) Theodosiou, M.; Widmaier, M.; Böttcher, R. T.; Rognoni, E.; Veelders, M.; Bharadwaj, M.; Lambacher, A.; Austen, K.; Müller, D. J.; Zent, R.; Fässler, R. Kindlin-2 Cooperates with Talin to Activate Integrins and Induces Cell Spreading by Directly Binding Paxillin. *eLife* **2016**, *5*, No. e10130.
(22) Zhang, X.; Jiang, G.; Cai, Y.; Monkley, S. J.; Critchley, D. R.; Sheetz, M. P. Talin Depletion Reveals Independence of Initial Cell Spreading from Integrin Activation and Traction. *Nat. Cell Biol.* **2008**, *10* (9), 1062−1068.
(23) Rahikainen, R.; Öhman, T.; Turkki, P.; Varjosalo, M.; Hytönen, V. P. Talin-Mediated Force Transmission and Talin Rod Domain Unfolding Independently Regulate Adhesion Signaling. *J. Cell Sci.* **2019**, No. jcs226514.
(24) Goult, B. T.; Brown, N. H.; Schwartz, M. A. Talin in Mechanotransduction and Mechanomemory at a Glance. *J. Cell Sci.* **2021**, *134* (20), No. jcs258749.
(25) Wang, Y.; Barnett, S. F. H.; Le, S.; Guo, Z.; Zhong, X.; Kanchanawong, P.; Yan, J. Label-Free Single-Molecule Quantification of Rapamycin-Induced FKBP-FRB Dimerization for Direct Control of Cellular Mechanotransduction. *Nano Lett.* **2019**, *19* (10), 7514−7525.
(26) Austen, K.; Ringer, P.; Mehlich, A.; Chrostek-Grashoff, A.; Kluger, C.; Klingner, C.; Sabass, B.; Zent, R.; Rief, M.; Grashoff, C. Extracellular Rigidity Sensing by Talin Isoform-Specific Mechanical Linkages. *Nat. Cell Biol.* **2015**, *17* (12), 1597−1606.
(27) Bodescu, M. A.; Aretz, J.; Grison, M.; Rief, M.; Fässler, R. Kindlin Stabilizes the Talin·integrin Bond under Mechanical Load by Generating an Ideal Bond. *Proc. Natl. Acad. Sci. U.S.A.* **2023**, *120* (26), No. e2218116120.
(28) Yu, M.; Le, S.; Barnett, S.; Guo, Z.; Zhong, X.; Kanchanawong, P.; Yan, J. Implementing Optogenetic Modulation in Mechanotransduction. *Phys. Rev. X* **2020**, *10* (2), No. 021001.
(29) Zabolocki, M.; McCormack, K.; van den Hurk, M.; Milky, B.; Shoubridge, A. P.; Adams, R.; Tran, J.; Mahadevan-Jansen, A.; Reineck, P.; Thomas, J.; Hutchinson, M. R.; Mak, C. K. H.; Añonuevo, A.; Chew, L. H.; Hirst, A. J.; Lee, V. M.; Knock, E.; Bardy, C. BrainPhys Neuronal Medium Optimized for Imaging and Optogenetics in Vitro. *Nat. Commun.* **2020**, *11* (1), 5550.
(30) Hansen, S. D.; Mullins, R. D. VASP Is a Processive Actin Polymerase That Requires Monomeric Actin for Barbed End Association. *J. Cell Biol.* **2010**, *191* (3), 571−584.
(31) Kanchanawong, P.; Shtengel, G.; Pasapera, A. M.; Ramko, E. B.; Davidson, M. W.; Hess, H. F.; Waterman, C. M. Nanoscale Architecture of Integrin-Based Cell Adhesions. *Nature* **2010**, *468* (7323), 580−584.
(32) Liu, J.; Wang, Y.; Goh, W. I.; Goh, H.; Baird, M. A.; Ruehland, S.; Teo, S.; Bate, N.; Critchley, D. R.; Davidson, M. W.; Kanchanawong, P. Talin Determines the Nanoscale Architecture of Focal Adhesions. *Proc. Natl. Acad. Sci. U.S.A.* **2015**, *112* (35), 4864−4873.
(33) Robertson, J.; Jacquemet, G.; Byron, A.; Jones, M. C.; Warwood, S.; Selley, J. N.; Knight, D.; Humphries, J. D.; Humphries, M. J. Defining the Phospho-Adhesome through the Phosphoproteomic Analysis of Integrin Signalling. *Nat. Commun.* **2015**, *6* (1), 6265.
(34) Case, L. B.; Baird, M. A.; Shtengel, G.; Campbell, S. L.; Hess, H. F.; Davidson, M. W.; Waterman, C. M. Molecular Mechanism of Vinculin Activation and Nanoscale Spatial Organization in Focal Adhesions. *Nat. Cell Biol.* **2015**, *17* (7), 880−892.
(35) Sadhanasatish, T.; Augustin, K.; Windgasse, L.; Chrostek-Grashoff, A.; Rief, M.; Grashoff, C. A Molecular Optomechanics Approach Reveals Functional Relevance of Force Transduction across Talin and Desmoplakin. *Sci. Adv.* **2023**, *9* (25), No. eadg3347.
(36) Erhart, D.; Zimmermann, M.; Jacques, O.; Wittwer, M. B.; Ernst, B.; Constable, E.; Zvelebil, M.; Beaufils, F.; Wymann, M. P. Chemical Development of Intracellular Protein Heterodimerizers. *Chem. Biol.* **2013**, *20*, 549−557.
(37) Ballister, E. R.; Aonbangkhen, C.; Mayo, A. M.; Lampson, M. A.; Chenoweth, D. M. Localized Light-Induced Protein Dimerization in Living Cells Using a Photocaged Dimerizer. *Nat. Commun.* **2014**, *5* (1), 5475.
(38) Bocker, J. K.; Friedel, K.; Matern, J. C.; Bachmann, A. L.; Mootz, H. D. Generation of a Genetically Encoded, Photoactivatable Intein for the Controlled Production of Cyclic Peptides. *Angew. Chem., Int. Ed.* **2015**, *54*, 2116−2120.
(39) Ruskowitz, E. R.; Munoz-Robles, B. G.; Strange, A. C.; Butcher, C. H.; Kurniawan, S.; Filteau, J. R.; DeForest, C. A. Spatiotemporal Functional Assembly of Split Protein Pairs through a Light-Activated SpyLigation. *Nat. Chem.* **2023**, *15* (5), 694−704.
(40) Andley, U. P.; Lewis, R. M.; Reddan, J. R.; Kochevar, I. E. Action Spectrum for Cytotoxicity in the UVA- and UVB-Wavelength Region in Cultured Lens Epithelial Cells. *Invest. Ophthalmol. Vis. Sci.* **1994**, *35* (2), 367−373.
(41) Tyrrell, R. M. Induction of Pyrimidine Dimers in Bacterial DNA by 365 nm Radiation. *Photochem. Photobiol.* **1973**, *17* (1), 69−73.
(42) Klak, M.; Gomółka, M.; Dobrzański, T.; Tymicki, G.; Cywoniuk, P.; Kowalska, P.; Kosowska, K.; Bryniarski, T.; Berman, A.; Dobrzyń, A.; Idaszek, J.; Święszkowski, W.; Wszoła, M. Irradiation with 365 and 405 nm Wavelength Shows Differences in DNA Damage of Swine Pancreatic Islets. *PLoS One* **2020**, *15* (6), No. e0235052.

https://doi.org/10.1021/jacs.3c07827
J. Am. Chem. Soc. XXXX, XXX, XXX−XXX

Supporting Figures

Visible light-induced specific protein reaction delineates early stages of cell adhesion

Rolle Rahikainen[a], Susan K. Vester[b,†], Paula Turkki[a], Chasity P. Janosko[c], Alexander Deiters[c], Vesa P. Hytönen[a] and Mark Howarth[b,d]

[a]Faculty of Medicine and Health Technology, Tampere University, Arvo Ylpön katu 34, 33520, Tampere, Finland and Fimlab Laboratories, Biokatu 4, 33520, Tampere, Finland.
[b]Department of Biochemistry, University of Oxford, South Parks Road, Oxford, OX1 3QU, UK.
[c]Department of Chemistry, University of Pittsburgh, Pittsburgh, PA 15260, United States.
[d]Department of Pharmacology, University of Cambridge, Tennis Court Road, Cambridge, CB2 1PD, UK.
[†]Present address: Randall Centre for Cell and Molecular Biophysics, King's College London, New Hunt's House, London, SE1 1UL, UK.

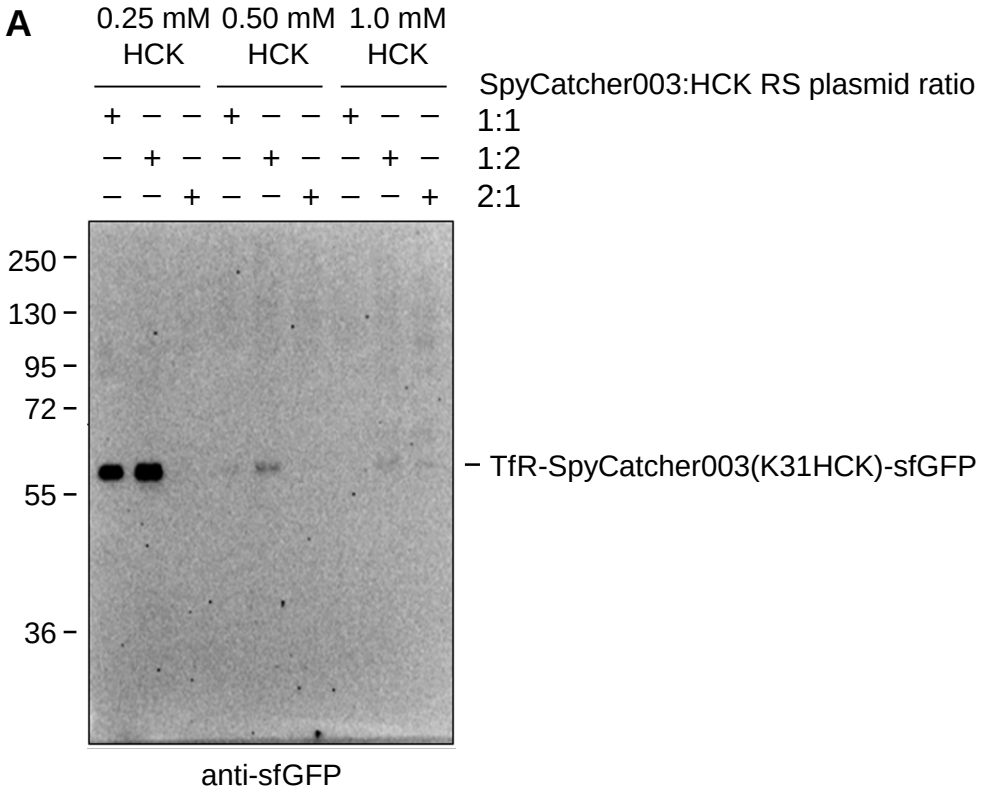

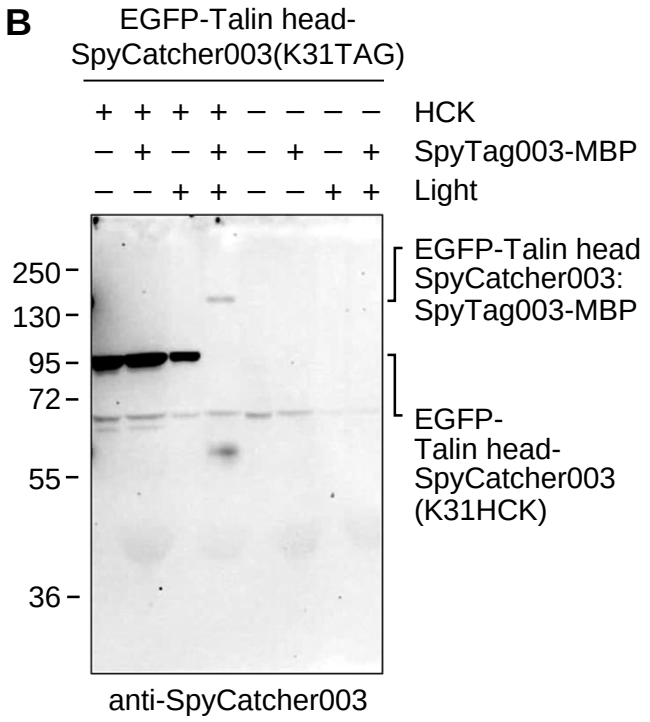

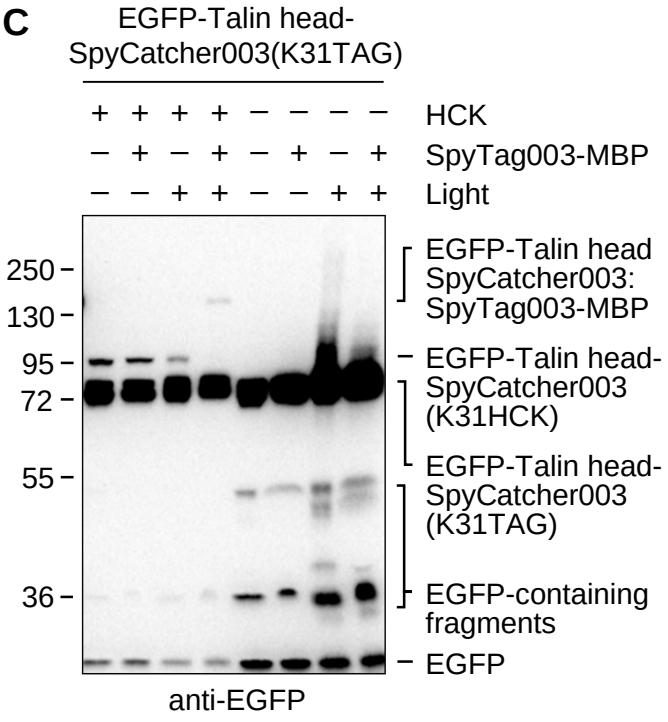

Figure S1. Validation of SpyCatcher003(K31HCK) photoactivation. (**A**) Titration of HCK concentration and plasmid ratios. HEK293T cells were transfected with different molar ratios of TfR-SpyCatcher003(K31TAG)-sfGFP and HCK RS plasmids and cultured in the presence of 0.25 mM – 1.0 mM HCK. Cell lysates were blotted for sfGFP, indicating successful incorporation of HCK in the polypeptide chain. (**B**) Photoactivation of covalent reactivity in EGFP-Talin head-SpyCatcher003(K31TAG) in cell lysates. Lysates of HEK293T cells transfected with EGFP-Talin head-SpyCatcher003(K31HCK) and HCK RS with or without HCK and light activation were mixed with recombinant SpyTag003-Maltose-binding protein (SpyTag003-MBP), before Western blotting with anti-SpyCatcher003. (**C**) As in panel B, but analyzed by Western blot against EGFP. GFP variants are highly stable to proteasomal degradation, so GFP-linked fragments are commonly observed to accumulate in cells.[54]

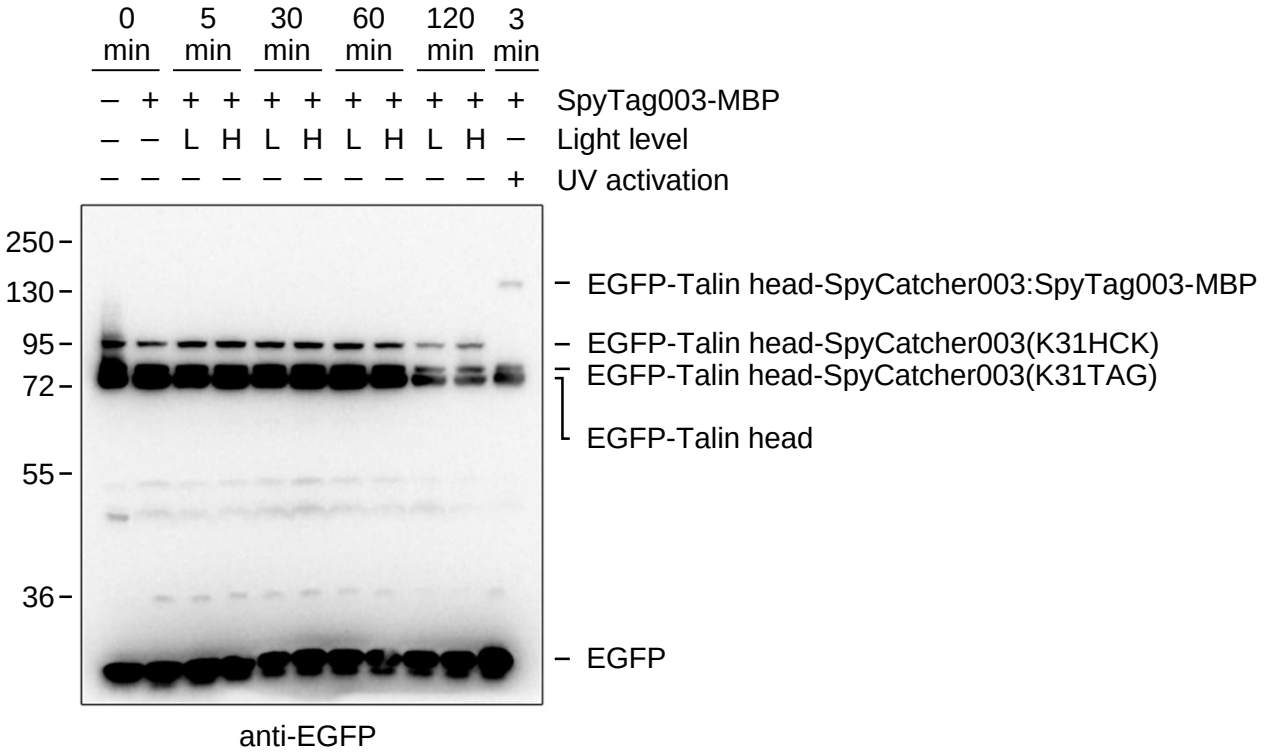

Figure S2. Photostability of SpyCatcher003(K31HCK) in ambient light. Photostability of SpyCatcher003(K31HCK) in typical laboratory lighting. Lysates of HEK293T cells expressing EGFP-Talin head-SpyCatcher003(K31HCK), HCK tRNAs and HCK RS were mixed with 50 μM SpyTag003-MBP and incubated for the indicated time, either in a dimly lit cold-room (Low intensity, L) or by the laboratory window (High intensity, H). The positive control sample was activated with a UV transilluminator. Analysis by Western blot against EGFP. As in Fig. S1, GFP variants are highly stable to degradation by the proteasome, so GFP-linked fragments are observed to accumulate in cells.[54]

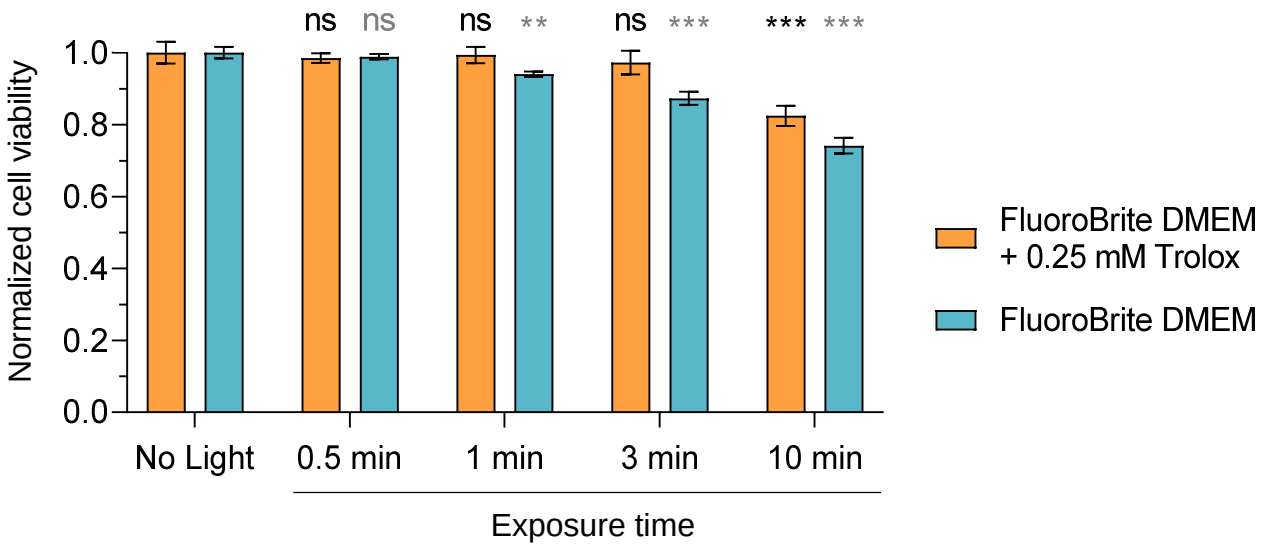

Figure S3. Assessment of potential phototoxicity from 405 nm illumination. Talin knock-out cells were cultured in FluoroBrite DMEM with Trolox (orange bars) or without (blue bars) and exposed to 405 nm wide-field light for the indicated time at 45 mW/cm^2, before resazurin-based cell viability assay. Viability is normalized to the No Light control, showing mean ± 1 SD for 3 replicates. Statistical comparisons against No Light control cells are shown for cells cultured with Trolox (black font) or no Trolox samples (gray font) using One-way ANOVA and Dunnett's test: *** $p<0.0001$, ** $p<0.001$, ns $p>0.05$.

A

SpyTag003	RGVPHIVMVDAYKRYK
SpyTag003(V114T, V116T)	RGVPHITMTDAYKRYK
SpyTag003(M115A)	RGVPHIVAVDAYKRYK
SpyTag003(M115G)	RGVPHIVGVDAYKRYK

Mutated residue

B

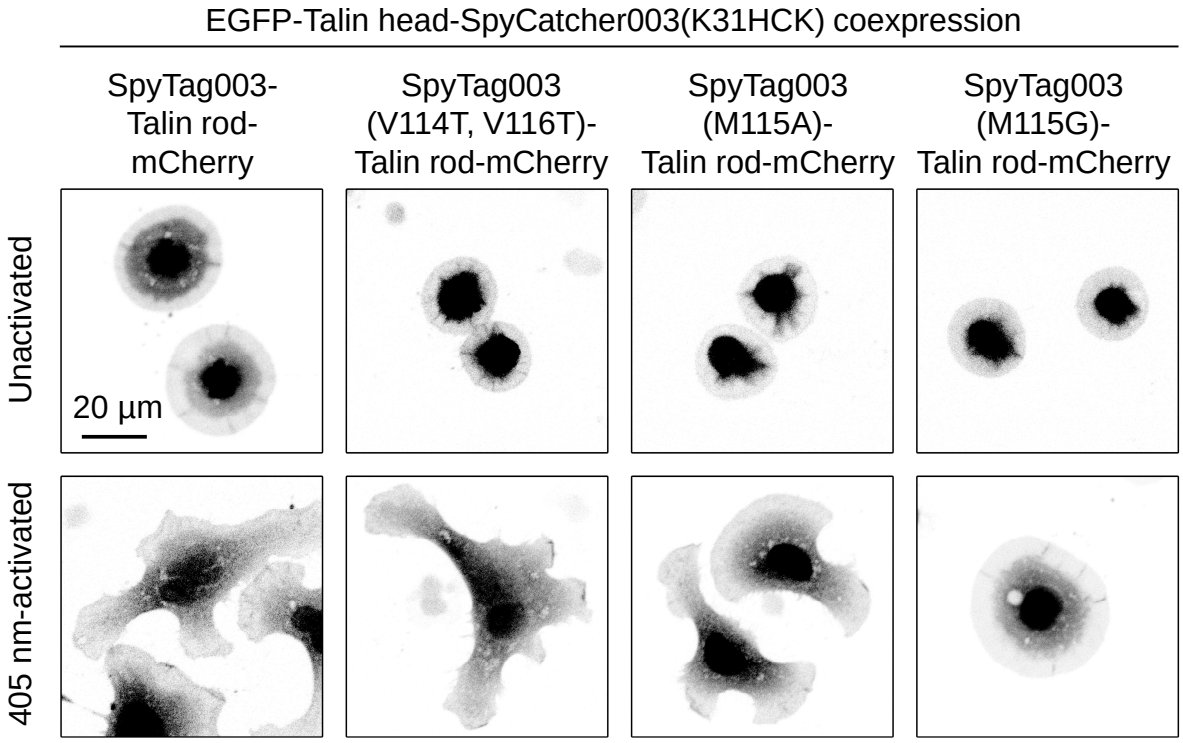

C

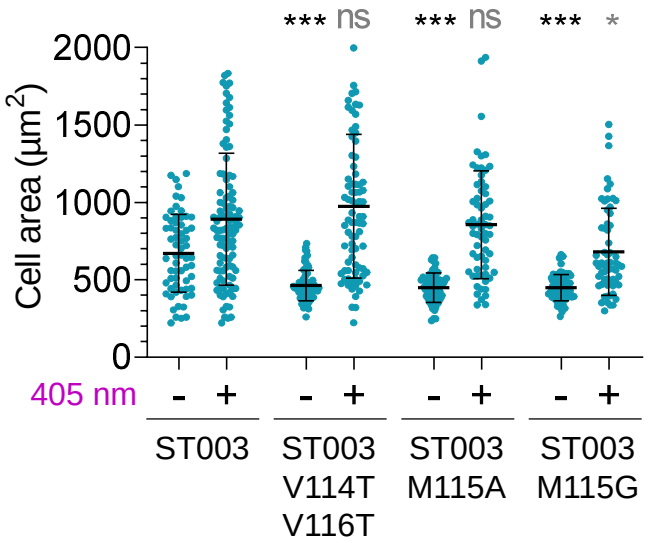

D

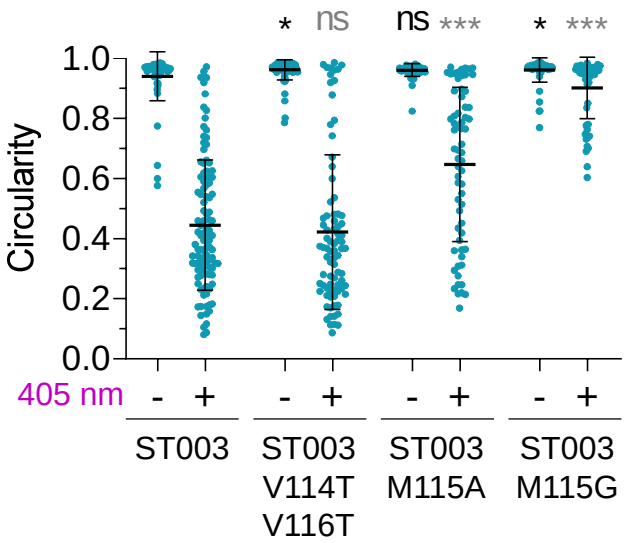

Figure S4. SpyTag003 mutants modify talin reconstitution after photoactivation. (**A**) SpyTag003 mutants designed to tune SpyCatcher003 covalent reconstitution. (**B**) Cell spreading and polarization after photoactivation. Talin knock-out cells expressing EGFP-Talin head-SpyCatcher003(K31HCK), variants of SpyTag003-Talin rod-mCherry, and HCK RS were activated for 1 min with 405 nm wide-field illumination, fixed after 90 min spreading, and imaged for EGFP by fluorescence microscopy. (**C-D**) Quantification of cell size and circularity following talin photoactivation as in B. Each blue circle is one cell, with black lines showing mean ± 1 SD. Mutants are compared with unactivated (black font) or 405 nm-activated (gray font) SpyTag003 cells using One-way ANOVA and Dunnett's test: *** $p<0.0001$, ** $p<0.001$, * $p<0.05$, ns $p>0.05$, n=62–106 cells. Data are representative of two experiments.

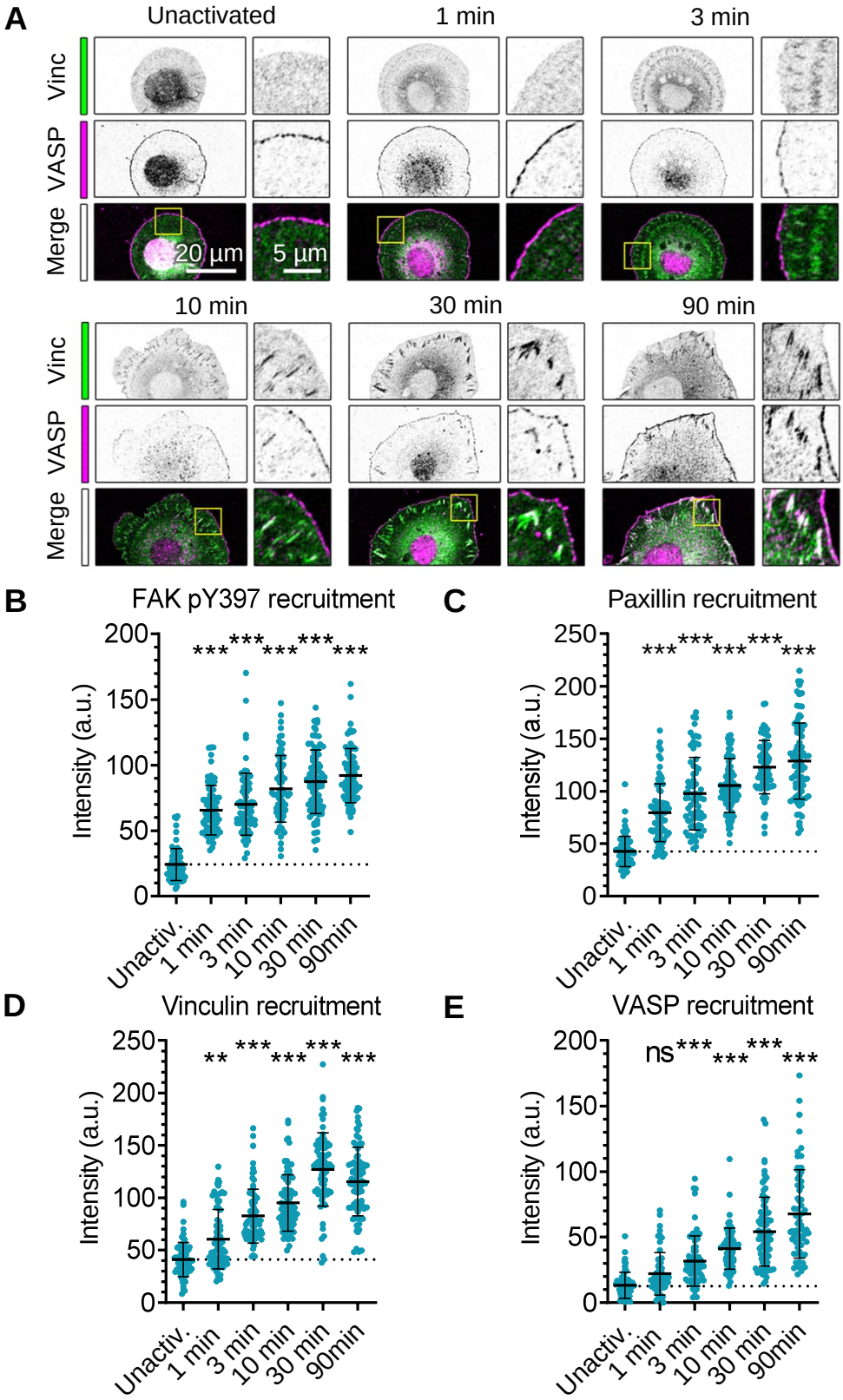

Figure S5. Time-course for adhesion assembly. (**A**) Vinculin and VASP recruitment after talin photoactivation. Talin knock-out cells were transfected as in Fig. 3E, activated at 405 nm and incubated for the indicated time. Cells were immunostained for VASP and vinculin. The yellow square is expanded in the right image. Vinculin and VASP are shown on their own in grayscale. Overlap of vinculin (green) and VASP (magenta) in the merge shows as white. (**B-E**) Recruitment of adhesion components following photoactivation. Raw adhesion intensities in arbitrary units (a.u.), to accompany normalized intensity in Fig. 3F. Each dot represents a single adhesion with mean ± 1 SD indicated as horizontal lines. FAK pY397: n = 75–81 adhesions in 15–16 cells. Paxillin: n = 70–86 adhesions in 14–17 cells. Vinculin: n = 74–81 adhesions in 12–15 cells. VASP: n = 60–86 adhesions in 12–15 cells. Results were pooled from two independent experiments. One-way ANOVA with Dunnett's test. *** $p < 0.0001$, ** $p < 0.001$, ns $p > 0.05$

Movie S1 legend.

Movie of split talin photoactivation in live cells. Talin knock-out cells were transfected with LifeAct-mNeonGreen, Talin head-SpyTag003, SpyCatcher003(K31HCK)-Talin rod-mScarletI and HCK RS and cultured with 0.25 mM HCK for 16–18 h. Left column shows inverted signal of actin labeling with LifeAct-mNeonGreen, middle column shows bright-field, and right column shows a merge of bright-field (grayscale) with LifeAct-mNeonGreen (green) determined by confocal microscopy. Top row: at 1 min 50 s, a circular 4-µm region was photoactivated by 405 nm illumination for 5 s, indicated by a magenta circle. Bottom row: cells treated in the same way but without 405 nm illumination. Photoactivation triggers initial local extension of the lamellipodium, followed by global cell spreading as reconstituted talin diffuses throughout the cell. The scale bar is 10 µm and the movie is shown at 6 frames per s (30-fold sped-up).

Visible light-induced specific protein reaction delineates early stages of cell adhesion

Methods

Plasmids and cloning

We used standard PCR methods with Q5 High-Fidelity 2× Master Mix (New England Biolabs) and Gibson assembly to perform cloning and site-directed mutagenesis. All open-reading frames were validated by Sanger sequencing (Source Bioscience). Residue numbers for SpyCatcher003 variants follow PDB ID: 2X5P.[43] Genscript plasmid cloning service was used to synthesize talin expression constructs for experiments in talin knock-out cells.

pcDNA3-mCherry-TAG-EGFP with one copy of *Desulfitobacterium hafniense* pyrrolysyl-$tRNA_{CUA}$ (PylT) with G8U under the control of a U6 promoter (1× U6-PylT) and one copy of *Methanosarcina barkeri* PylT with U25C under the control of a H1 promoter (1× H1-PylT) has been described.[44] *D. hafniense* PylT G8U mutation restores canonical U8-A14 interaction and *M. barkeri* PylT U25C mutation stabilizes the anticodon stem and slightly increases amino acid incorporation efficiency.[45,46] pcDNA3-EGFP-Talin head-SpyCatcher003 and pcDNA3-EGFP-Talin head-SpyCatcher003(K31TAG) (GenBank OR711469, Addgene ID 210023) with 1× U6-PylT and 1× H1-PylT were derived from pcDNA3-mCherry-TAG-EGFP and pEGFP-C1-EGFP-Talin head-SpyCatcher003 (GenBank MN527523, Addgene ID 133566),[47] which have been described. Talin head comprises amino acids 1-433 of mouse talin-1. The amber stop codon TAG instead of the lysine at position 31 of SpyCatcher003 allows for the incorporation of 7-hydroxycoumarin-caged lysine (HCK) when co-expressed with HCK tRNA synthetase (HCK RS) and PylT.

pcDNA3-TfR-SpyCatcher003-superfolder green fluorescent protein (sfGFP) and pcDNA3-TfR-SpyCatcher003(K31TAG)-sfGFP-MycTag-CTag (GenBank OR711470, Addgene ID 210021) with 1× U6-PylT and 1× H1-PylT were derived from pcDNA3-mCherry-TAG-EGFP and pENTR4-TfR-sfGFP-SpyCatcher003 (GenBank MN433890, Addgene ID 133451),[47] which have been described. TfR comprises the Transferrin receptor transmembrane domain and cytosolic region with Y20C and F23A mutations to block internalization and allows for mammalian cell surface expression of SpyCatcher003.[47] In this context, sfGFP should only be expressed when HCK has successfully been incorporated in the growing polypeptide chain.

pcDNA3-LifeAct-mNeonGreen-IRES-Talin head-SpyTag003 (GenBank OR711471, Addgene ID 210024) with 1× U6-PylT and 1× H1-PylT was derived from pcDNA3-EGFP-Talin head-SpyCatcher003 and encodes mouse codon-optimized LifeAct-mNeonGreen, followed by encephalomyocarditis virus (EMCV) internal ribosome entry site (IRES) and Talin head-SpyTag003. pcDNA3-Talin head-SpyTag003 was derived from pcDNA3-LifeAct-mNeonGreen-IRES-Talin head-SpyTag003 by removing the cassette encoding LifeAct-mNeonGreen and IRES. pEGFP-C1 SpyCatcher003(K31TAG)-Talin rod (434-2541)-mScarletI (GenBank OR711472, Addgene ID 210022), pEGFP-C1 SpyTag003(V114T, V116T)-Talin rod (434-2541)-mCherry (Addgene ID 210027), pEGFP-C1 SpyTag003(M115A)-Talin rod (434-2541)-mCherry (Addgene ID 210025) and pEGFP-C1 SpyTag003(M115G)-Talin rod (434-2541)-mCherry (Addgene ID 210026) were derived from pEGFP-C1 SpyTag003-Talin rod (434-2541)-mCherry (GenBank MN527524 and Addgene ID 133567) previously described.[47] In the context of pEGFP-C1 SpyCatcher003(K31TAG)-Talin rod (434-2541)-mScarletI, mScarletI should only be expressed when HCK has successfully been incorporated in the growing polypeptide chain.

pE323-HCK RS contains the engineered HCK tRNA synthetase with five copies of PylT from *Methanosarcina mazei* with U25C under the control of a U6 promoter (5× U6-PylT) and has been described.[48] pET28a-SpyTag003-MBP (GenBank MN433888, Addgene ID 133450) has been previously described.[47]

Hydroxycoumarin-caged lysine

HCK was synthesized as previously described[49] and made up at 100 mM in DMSO. HCK stock was stored at -20 °C protected from light and directly added into cell culture medium after transfection. For all No-HCK control samples, an equal volume of DMSO was added. To minimize the possibility of premature photoreaction, handling of HCK was performed under low light conditions in a tissue culture hood (with the hood light off and the room lights dimmed). During assays, HCK-incorporated samples were handled at ambient light but protected with aluminum foil and/or placed in a closed polystyrene ice box during incubations and waiting times.

To avoid possible phototoxicity of reactive oxygen species in the 405 nm activation of HCK in living cells, 0.25 mM Trolox (Sigma-Aldrich) was added as an antioxidant.[50] 100 mM stock of Trolox was prepared in 99.7 % (v/v) ethanol and stored at 4 °C.

Expression of caged SpyCatcher003 in HEK293T cells

HEK293T cells were maintained in complete Dulbecco's Modified Eagle Medium [DMEM (Sigma-Aldrich) supplemented with 10% (v/v) fetal bovine serum (FBS, Sigma-Aldrich), as well as 50 U/mL penicillin and 50 µg/mL streptomycin (Thermo Fisher)] under humidified conditions at 37 °C and 5% (v/v) CO_2. The day before transfection, 250,000 HEK293T cells were seeded in 2 mL complete DMEM in 6-well plates (Greiner). Cells were transfected with 2 µg plasmid DNA (1 part pcDNA3-EGFP-Talin head-SpyCatcher003 WT/K31TAG and 2 parts pE323-HCK RS) using 2 µL jetOPTIMUS (Polyplus) according to the manufacturer's instructions. HCK was added to a final concentration of 0.25 mM after transfection. For control wells, 0.25% (v/v) DMSO was added. Cells were grown for 48 h, before Western blot analysis with the plates wrapped in aluminum foil.

HEK293T cell lysis

HEK293T cells in 6-well plates were washed three times with 1 mL phosphate-buffered saline (PBS: 137 mM NaCl, 2.7 mM KCl, 10 mM Na_2HPO_4, 1.8 mM KH_2PO_4, pH 7.4), then incubated in 200 µL ice-cold lysis buffer [25 mM Tris-HCl pH 7.5 (pH adjusted at 25 °C) + 150 mM NaCl + 5% (v/v) glycerol + 1% (v/v) Triton X-100, supplemented with cOmplete Mini EDTA-free Protease Inhibitor Cocktail (Roche) and 1 mM phenylmethylsulfonylfluoride (PMSF, Thermo Fisher)] for 10 min on ice in a closed ice box. The cells were scraped off, transferred to 1.5 mL tubes and centrifuged at 20,000 g for 10 min at 4 °C. The supernatant was used immediately or stored at -20 °C. Protein concentrations were determined by bicinchoninic acid assay (BCA Protein Assay Kit, Thermo Fisher) in 96-well format using 5 µL cell lysate diluted with 5 µL lysis buffer and correcting for lysis buffer, with bovine serum albumin (BSA) standards at 0, 125, 250, 500, 750, 1000, 1,500 or 2,000 µg/mL. Incubation with 200 µL BCA working solution was performed at 37 °C for 30 min. A_{562} measurement was performed using a FLUOstar Omega plate reader with FLUOstar Omega software version 5.10 R2 (both BMG Labtech) at 25 °C.

Talin knock-out cell lysis

Tln1$^{-/-}$*Tln2*$^{-/-}$ mouse kidney fibroblasts were a kind gift from Prof. Carsten Grashoff, University of Münster, and have been previously described.[51] Briefly, mice carrying *loxP* flanked *Tln1* alleles (*Tln1*$^{flox/flox}$) were crossed with a mouse strain with nullizygous *Tln2* alleles (*Tln2*$^{-/-}$).

Kidney fibroblasts were isolated from the resulting *Tln1*$^{flox/flox}$ *Tln2*$^{-/-}$ mice and immortalized by retroviral transduction of SV40 large T antigen. Adenoviral transduction of Cre recombinase was used to delete the floxed *Tln1* alleles.[51] Talin knock-out cells were maintained in complete FluoroBrite medium [FluoroBrite DMEM (A1896701, Thermo Fisher) supplemented with 10% (v/v) FBS (10270106, Gibco) and 1% (v/v) GlutaMax (35050061, Thermo Fisher)] under humidified conditions at 37 °C and 5% (v/v) CO_2. The cell-line was regularly tested for mycoplasma contamination.

For immunoblotting in Fig. 1E, Talin knock-out cells cultured on 60 mm dishes were briefly washed with PBS and lysed with 150 µL of 5× SDS-PAGE sample buffer: 250 mM Tris-HCl, pH 6.8, 10% (w/v) SDS, 30% (v/v) glycerol, 0.02% (w/v) bromophenol blue, 25 mM tris(2-carboxyethyl)phosphine (TCEP). Lysed cells were collected to the dish corner with cell scrapers and the lysate was transferred to 1.5 mL tubes cooled on ice. Samples were heated for 5 min at 95 °C, briefly spun down to collect liquid, and stored at -20 °C before blotting.

Initial optimization of caged SpyCatcher003 expression in HEK293T cells

Optimization was performed in 24-well plates (Greiner). HEK293T cells were seeded at 50,000 cells/mL in 0.5 mL complete DMEM. Cells were transfected with 0.25 µg total DNA using 0.25 µL jetOPTIMUS, at molar ratios 1:1, 1:2 and 2:1 [pcDNA3-TfR-SpyCatcher003(K31TAG)-sfGFP to pE323-HCK RS]. Directly after transfection, HCK was added to a final concentration of 0.25 mM, 0.5 mM or 1 mM. Western blot analysis was performed 48 h after transfection. For lysis, HEK293T cells were washed three times with 0.5 mL PBS, then incubated in 75 µL ice-cold lysis buffer and processed as described above.

Protein purification by Ni-NTA

SpyTag003-MBP was expressed in *E. coli* EXPRESS BL21(DE3) (Lucigen) and purified by Ni-NTA at 4 °C. Bacterial cell pellets of SpyTag003-MBP were resuspended in Ni-NTA buffer (50 mM Tris-HCl pH 7.8 + 300 mM NaCl) supplemented with cOmplete Mini EDTA-free Protease Inhibitor Cocktail (Roche) and 1 mM PMSF. Cells were lysed by sonication on ice at 50% duty cycle for 4 × 1 min with 1 min rest between runs. Cell lysates were clarified by centrifugation at 30,000 g for 30 min at 4 °C, then incubated with Ni-NTA agarose (Qiagen) for 1 h at 4 °C with rolling. Resin was pelleted by centrifugation, then washed with 20 column volumes (CV) of Ni-NTA buffer and Ni-NTA wash buffer (50 mM Tris-HCl + 300 mM NaCl + 10 mM imidazole at pH 7.8). The resin was transferred to Econo-Pac Chromatography Columns (Bio-Rad) and washed with a further 20 CV of Ni-NTA wash buffer by gravity flow. Elution was performed with Ni-NTA elution buffer (50 mM Tris-HCl + 300 mM NaCl + 200 mM imidazole at pH 7.8) by incubating the resin with 4 × 1 CV for 5 min. SpyTag003-MBP was dialyzed into PBS in three dialysis steps using 3.5 kDa molecular weight cut-off (MWCO) dialysis tubing (Spectrum Labs). Protein concentrations were determined by A_{280} measurement on a NanoDrop One (Thermo Fisher) using NanoDrop One software version 1.4.2, with extinction coefficients predicted by ExPASy ProtParam.[52]

Intracellular 405 nm uncaging for Western blot

Talin knock-out cells were transfected with pcDNA3-EGFP-Talin head-SpyCatcher003(K31TAG), pEGFP-C1 SpyTag003-Talin rod (434-2541)-mCherry and HCK RS plasmids as described below, and plated on a 60 mm dish at 2×10^6 cells per dish. After an initial 2 h recovery phase at 37 °C and 5% (v/v) CO_2, FluoroBrite DMEM was replaced with FluoroBrite DMEM supplemented either with 0.25 mM HCK (100 mM stock in DMSO) and 0.25 mM Trolox or with 0.25 % DMSO and 0.25 mM Trolox. Incubation at 37 °C and 5% (v/v) CO_2 was continued for 17 h, after which cells were washed twice with FluoroBrite DMEM supplemented with 0.25 mM Trolox and incubated at 37 °C and 5% (v/v) CO_2 for 15 min. For

intracellular SpyCatcher003(HCK) uncaging, culture dishes were placed for 1 min on 2 × 6 W 405 nm LED panels (Sovol) with total intensity of 45 mW/cm^2 at the plane of cells. Activated cells were allowed to recover at 37 °C and 5% (v/v) CO_2 for 5 min and the activation cycle was repeated two more times for a total activation time of 3 min. Cells were incubated at 37 °C and 5% (v/v) CO_2 for 1h 30 min and lysed for Western blot as described below.

Uncaging and reaction of SpyCatcher003 in cell lysates

Equal amounts of protein lysates as determined by BCA assay were transferred to PCR tubes. To test spontaneous uncaging by ambient light, samples were incubated exposed to room light in a cold room or next to a window on ice for the indicated amounts of time. For uncaging, designated samples were irradiated on a ChemiDoc XRS+ using the Ethidium Bromide setting for the indicated amounts of time at 25 °C. Samples were transferred back to ice to chill and incubated with 50 µM SpyTag003-MBP at 4 °C for 1 h. Reaction was stopped by mixing with 6× SDS loading buffer [234 mM Tris-HCl pH 6.8, 24% (v/v) glycerol, 120 µM bromophenol blue, 234 mM SDS, supplemented with 60 mM dithiothreitol (DTT) for reduced samples] and heating at 95 °C for 5 min in a Bio-Rad C1000 thermal cycler.

Western blot

SDS-PAGE in Fig. 1E was performed using Bio-Rad Mini-PROTEAN Tetra Vertical Electrophoresis Cell with Bio-Rad 4-15% Mini-PROTEAN TGX Precast gels. Gels were run with in 24 mM Tris base, 192 mM glycine, 3.5 mM SDS at 120 V. Proteins were transferred to nitrocellulose membranes using Bio-Rad Trans-Blot Turbo Transfer System at 1.3 A and 25 V for 10 min. Membranes were blocked with Bio-Rad EveryBlot blocking solution for 1 h 30 min at 25 °C. Anti-EGFP antibody (SICGEN ab0020) was diluted 1:1,000 and anti-mScarlet (also recognizing mCherry) antibody (SICGEN ab9088) was diluted 1:2,000 directly into the blocking solution. Primary antibodies were incubated for 16 h at 4 °C with gentle agitation. Membranes were washed four times in 0.05% TBST [50 mM Tris-HCl, 150 mM NaCl, pH 7.4 + 0.05% (v/v) Tween 20] for 5 min at 25 °C. Secondary antibody detection was performed by staining for 1 h 30 min at 25 °C with Licor IRDye 680RD donkey anti-goat IgG (Licor 926-68074) diluted 1:20,000 into Bio-Rad EveryBlot blocking buffer. Membranes were washed five times in 0.05% TBST before a final wash with TBS. Membranes were imaged using Licor CLx imager with 84 µm resolution and medium image quality.

SDS-PAGE in Fig. S1A-C and Fig. S2 was performed using an XCell SureLock system (Thermo Fisher) with 10% (w/v) polyacrylamide gels. Gels were run in 24 mM Tris base, 192 mM glycine, 3.5 mM SDS at 200 V. Proteins were transferred onto nitrocellulose membranes by dry transfer using an iBlot 2 gel transfer device (Thermo Fisher) at 25 V for 10 min. Membranes were blocked for 1 h at 25 °C in 5% (w/v) skimmed milk in PBS. The primary antibody was diluted in 2.5% (w/v) skimmed milk in 0.05% PBST [PBS + 0.05% (v/v) Tween 20], with mouse anti-GFP (Thermo Fisher, MA5-15256, clone GF28R) at 1:2,000 or mouse anti-SpyCatcher003 serum[53] at 1:300. Incubation was performed overnight at 4 °C. Membranes were washed three times in 0.1% PBST [PBS + 0.1% (v/v) Tween 20] for 5 min at 25 °C. Secondary antibody detection was performed by staining with goat anti-mouse IgG Horseradish Peroxidase (Sigma-Aldrich, A4416) at 1:5,000 for 1 h at 25 °C in 2.5% (w/v) skimmed milk in 0.05% PBST. After three further washes in 0.1% PBST and one wash in PBS at 25 °C, membranes were developed at 25 °C with SuperSignal West Pico Plus Chemiluminescent Substrate (Thermo Fisher) and imaged using a ChemiDoc XRS+ imager (Bio-Rad). In immunoblotting with anti-EGFP antibody, we observed EGFP-containing degradation products of EGFP-Talin head-SpyCatcher003(K31TAG), consistent with reported high stability of EGFP in cells.[54] A colon is used to indicate products linked by Tag/Catcher isopeptide bond formation.

Expression of caged SpyCatcher003 in talin knock-out cells
Talin knock-out cells were transiently transfected with Neon Transfection System electroporator (Thermo Fisher) according to the manufacturer's instructions. Briefly, 10^6 cells in 100 µL were transfected with 12.5 µg of total plasmid DNA at 2:2:1 molar ratio of pE323-HCK RS, SpyCatcher003(K31TAG)-Talin rod (434-2541)-mScarletI and Talin head-SpyTag003 plasmids, respectively. The electroporation parameters were 1,400 V, 30 ms and 1 pulse.

Phototoxicity assay for 405 nm wide-field activation
Talin knock-out cells were plated on Nunclon Delta-Treated 96-well plates (Nunc) at 50,000 cells per well. Cells were incubated at 37 °C and 5% (v/v) CO_2 for 1 h in 100 µL FluoroBrite DMEM (Thermo Fisher) supplemented with either 0.25 mM Trolox (Sigma-Aldrich, 100 mM stock in ethanol) or matching ethanol concentration at 0.25 % (v/v). Cells were exposed to 405 nm light (45 mW/cm^2) from a wide-field LED light source for 0.5-10 min and allowed to recover for 15 min at 37 °C and 5% (v/v) CO_2. 20 µL resazurin-based CellTiter-Blue reagent (Promega) was added per well, before the plates were gently mixed and incubated for 4 h at 37 °C and 5% (v/v) CO_2. Plates were cooled to 21 °C and 80 µL samples of culture media were transferred to black half-area microplates (Nunc). Media fluorescence at 550 nm excitation wavelength and 590 nm emission wavelength was measured using a Tecan Spark microplate reader. The linearity of CellTiter-Blue fluorescence signal at the used cell density and incubation time was confirmed with control experiments. Media-only controls with FluoroBrite DMEM supplemented with either 0.25 mM Trolox or 0.25% (v/v) ethanol and exposed for 0-10 min at 405 nm were used to correct results for changes in media fluorescence. All results were normalized by the fluorescence of unexposed cells cultured in matching media conditions.

Live-cell imaging and on-stage 405 nm photoactivation
Zeiss high-performance 170 µm-thick coverslips were washed with 2% (v/v) Hellmanex-III (Sigma-Aldrich) in a bath sonicator at 40 °C for 20 min (Finnsonic), rinsed with deionized water, and sonicated again in 96% (v/v) ethanol. Coverslips were rinsed with deionized water, air-dried, and attached to perforated 35 mm polystyrene dishes (MatTek). Attached coverslips were coated with 25 µg/mL human fibronectin in PBS for 30 min at 37 °C and washed twice with PBS. Fibronectin was purified from human plasma preparate (Octaplas) using gelatin affinity chromatography (Gelatin Sepharose 4B; GE Healthcare) as previously described.[55]

Transfected talin knock-out cells were plated on glass bottom dishes (166,000 cells per dish) in 120 µL complete FluoroBrite medium and were incubated at 37 °C and 5% (v/v) CO_2 for 1 h to allow cell attachment. Dishes were filled with complete FluoroBrite medium and the incubation at 37 °C and 5% (v/v) CO_2 continued for 2 h. Media was replaced with 800 µL of FluoroBrite-Trolox-HCK (complete FluoroBrite medium supplemented with 0.25 mM Trolox and 0.25 mM HCK) and cells were incubated at 37 °C and 5% (v/v) CO_2 for 16-18 h. Before imaging, media was replaced with FluoroBrite-Trolox (complete FluoroBrite medium supplemented with 0.25 mM Trolox) and the dish was mounted to a humified 37 °C and 5% (v/v) CO_2 incubator on the microscope stage.

For live-cell imaging and on-stage 405 nm photoactivation, we used a Nikon Eclipse Ti2-E inverted microscope equipped with A1R+ laser scanning confocal (Nikon), Perfect Focus System (Nikon) and Nikon SR HP Plan Apo 100×/1.35 Silicone immersion objective. Single cells were imaged at 80 nm pixel size and 67.7 µm pinhole size using 488 nm solid state laser (0.25 - 0.5% laser) for mNeonGreen excitation and 561 nm solid state laser (0.2 - 0.5% laser) for mScarletI excitation. We used 560 nm long-pass dichroic mirror and 525/50 nm band-

pass filter for mNeonGreen emission and 640 nm long-pass dichroic mirror and 595/50 nm band-bass filter for mScarletI emission.

Differential Interference Contrast (DIC) images were captured using transmitted 488 nm excitation light. Images were captured at 5 s intervals for 23 images before photoactivation. For HCK photoactivation, a circular region of 4.0 µm was activated for 5 loops (4.8 s total) with 10.5 µW (5%) 405 nm laser. Imaging was then immediately continued for 73 images at 5 s intervals.

"Unactivated" cells were cultured with HCK but not 405 nm activated. In Fig. 3, "No HCK" cells were cultured without HCK, activated with 405 nm, and allowed to spread for 90 min. When green and magenta images are merged, the overlapping regions appear white.

Lamellipodium extension analysis

Fiji distribution of ImageJ 1.53t[56] was used to analyze lamellipodium extension after HCK photoactivation. A 10-pixel (0.8 µm) wide line perpendicular to the cell edge was drawn across the cell lamellipodium at the site of photoactivation. A kymograph of mNeonGreen intensity was created along this line, covering all 96 frames of the time-series. Using free-hand selection tool, the movement of the lamellipodium edge over time was traced in the kymograph by following the shift in the position of mNeonGreen intensity. The selection created in this way was used to quantify the number of pixels above the line (inside cell) and below the line (outside cell) for all columns of pixels, each representing a single image captured at 5 s intervals. For relative lamellipodium extension, the results were normalized with the initial position of the lamellipodium edge. To calculate the lamellipodium extension rate, sharp irregularities in the extension data were smoothed by averaging with a 4-frame sliding window and the rate of change over time was calculated.

Actin flow-rate analysis

To improve the clarity of LifeAct-mNeonGreen live-cell imaging data, Huygens Essential 23.04 (Scientific Volume Imaging) with classic maximal likelihood estimation (CMLE) deconvolution algorithm was used. Deconvoluted images were analyzed using Fiji distribution of ImageJ 1.53t.[56] Briefly, at the site of photoactivation, a 20-pixel (1.6 µm) wide line perpendicular to the cell edge was drawn across the lamellipodium to create 5 parallel kymographs, each representing the mean intensity of 4 pixels in the original image. These kymographs were used to measure manually the slope of actin flow at 30 s intervals (6-pixel spacing in the kymographs) using the line selection tool. Of the 5 parallel kymographs, at each time-point, the one with the best image clarity was selected for analysis. The slopes measured in this way were used to calculate actin flow rate (nm/s) using trigonometry.

Widefield 405 nm activation of talin knock-out cells

Transfected talin knock-out cells were plated on 60 mm dishes (Nunc) in complete FluoroBrite medium and allowed to recover for 3 h at 37 °C and 5% (v/v) CO_2. The media was replaced with FluoroBrite-Trolox-HCK and the incubation at 37 °C and 5% (v/v) CO_2 was continued for 16-18 h. After the addition of FluoroBrite-Trolox-HCK, all subsequent culture steps were performed in low light conditions. Cells were rinsed with PBS, detached using TrypLE Express (Thermo Fisher) and plated in FluoroBrite-Trolox-HCK on fibronectin coated glass-bottom dishes, prepared as described above. After 1 h incubation at 37 °C and 5% (v/v) CO_2, cells were rinsed once with FluoroBrite-Trolox and incubated at 37 °C and 5% (v/v) CO_2 for 15 min to wash out residual HCK. For HCK uncaging, dishes were placed on top of 2 × 6 W 405 nm LED panels (Sovol) with 45 mW/cm^2 total intensity and photoactivated for 60 s. Photoactivated cells were incubated at 37 °C and 5% (v/v) CO_2 and fixed at defined timepoints. For fixation,

media was aspirated and 4% (w/v) paraformaldehyde in PBS was added for 20 min at 22 °C. Cells were washed 4 times with PBS and stored at 4 °C.

Immunostaining

Fixed cells were permeabilized with 0.2% (v/v) Triton X-100 in PBS for 5 min at 22 °C. Non-specific antibody binding was inhibited with blocking buffer [5% (v/v) fetal calf serum (Gibco), 1% (w/v) bovine serum albumin (Sigma-Aldrich) and 0.05% (v/v) Triton X-100 (Sigma-Aldrich) in PBS] for 30 min at 22 °C. Primary antibodies were diluted in the blocking buffer and incubated for 90 min at 22 °C with 1:400 anti-vinculin V9131 (Sigma-Aldrich, RRID:AB_477629), 1:100 anti-VASP HPA005724 (Sigma-Aldrich, RRID:AB_1858721), 1:200 anti-FAK pY397 ab81298 (Abcam, RRID:AB_1640500), or 1:100 anti-paxillin BD610051 (BD Biosciences, RRID:AB_397463). Cells were washed 4 times for 10 min with PBS. Fluorescently-labeled secondary antibodies were diluted in the blocking buffer at 1:250 and incubated on samples for 90 min: Goat anti-Mouse IgG (H+L) AlexaFluor Plus 488 A32723 (Thermo Fisher, RRID:AB_2633275), Goat anti-Rabbit IgG (H+L) AlexaFluor Plus 488 A32731 (Thermo Fisher, RRID:AB_2633280), Goat anti-Mouse IgG (H+L) AlexaFluor Plus 647 A32728 (Thermo Fisher, RRID:AB_2633277), Goat anti-Rabbit IgG (H+L) AlexaFluor Plus 647 A32733 (Thermo Fisher RRID:AB_2633282). Cells were washed 4 times for 10 min with PBS and covered with a clean coverslip using Prolong Glass antifade mounting media (Thermo Fisher). The mounting media was cured at 24 °C for a minimum of 40 h before imaging.

Cell size and morphology analysis

For cell size and morphology analysis, mScarletI signal of fixed samples was imaged using a Nikon Eclipse Ti2-E inverted microscope equipped with A1R+ laser scanning confocal unit (Nikon) and Nikon Apo 60×/1.40 Oil λS DIC N2 objective. For *No HCK* samples (Fig. 3B,C) not expressing mScarletI because of polypeptide chain termination, anti-vinculin antibody staining was imaged instead.

Cell area and circularity were analyzed in Fiji distribution of ImageJ 1.53t[56] using the free-hand selection tool to trace cell boundaries. Cell circularity was calculated with the formula: circularity = $4\pi(\text{area}/\text{perimeter}^2)$. Cells with partially detached lamellipodium or extremely high mScarletI signal were excluded from the analysis. For each timepoint, 45 to 110 cells from 2 independent experiments were analyzed.

Adhesion intensity analysis

For adhesion intensity analyses, immunostained cells were imaged using a Zeiss Axio Observer.Z1 equipped with Zeiss LSM800 laser scanning confocal unit and Zeiss Plan-Apochromat 63×/1.40 oil immersion objective. 107 µm × 107 µm fields were imaged at 70 nm pixel size and 200 nm Z-stack interval, maintaining fixed laser intensities and detector gains for all samples.

Adhesion protein localization to adhesion sites was analyzed using Fiji distribution of ImageJ 1.53t.[56] The Z-stack slices with the highest adhesion/cytosol contrast were selected for the analysis. For each cell, the 5 adhesions with the highest fluorescence intensity were masked using the freehand selection tool and the mean intensity of each selected region was measured. For each image, the intensity of background control region outside the cell was measured and its intensity value was subtracted from all adhesion intensity values of the same image. For Fig. 3F, adhesion intensity values were normalized by the mean intensity measured at the 90 min timepoint. For unactivated cells, no clear adhesion structures were observed and the reported intensity values represent mean lamellipodium intensity. For each adhesion protein, 60-85 adhesions in 12-17 cells from two independent experiments were analyzed. Statistical

significance of results was tested using one-way ANOVA with Dunnett's post-test in GraphPad Prism 9.0.0 (GraphPad Software). All other samples were compared with the unactivated samples. p-values below 0.05 were considered statistically significant. p-values above 0.05 were considered non-significant (ns). Samples in the same experiment were prepared, imaged and analyzed under uniform conditions.

Visualization of structural models and reaction schematics

The structural model for SpyTag/SpyCatcher is based on PDB ID 4MLI[57] and visualized in PyMOL version 2.2.2 (Schrödinger). SpyTag/SpyCatcher reaction was drawn in ChemSketch 2022.2.3 (ACD/Labs) and HCK uncaging reaction in ChemDraw 20.1.1.125 (PerkinElmer).

Data availability

Sequences of constructs are available in GenBank, as described in the section "Plasmids and Cloning". Indicated plasmids have been deposited in the Addgene repository (https://www.addgene.org/Vesa_Hytonen/). Further information and request for resources and reagents should be directed to and will be fulfilled by the lead contact, M.H. (mh2186@cam.ac.uk). Requests for unnatural amino acid resources should be directed to A.D. (deiters@pitt.edu).

References

(43) Oke, M.; Carter, L. G.; Johnson, K. A.; Liu, H.; McMahon, S. A.; Yan, X.; Kerou, M.; Weikart, N. D.; Kadi, N.; Sheikh, M. A.; Schmelz, S.; Dorward, M.; Zawadzki, M.; Cozens, C.; Falconer, H.; Powers, H.; Overton, I. M.; Van Niekerk, C. A. J.; Peng, X.; Patel, P.; Garrett, R. A.; Prangishvili, D.; Botting, C. H.; Coote, P. J.; Dryden, D. T. F.; Barton, G. J.; Schwarz-Linek, U.; Challis, G. L.; Taylor, G. L.; White, M. F.; Naismith, J. H. The Scottish Structural Proteomics Facility: Targets, Methods and Outputs. *J. Struct. Funct. Genomics* **2010**, *11* (2), 167–180. https://doi.org/10.1007/s10969-010-9090-y.

(44) Zhou, W.; Wesalo, J. S.; Liu, J.; Deiters, A. Genetic Code Expansion in Mammalian Cells: A Plasmid System Comparison. *Bioorg. Med. Chem.* **2020**, *28* (24), 115772. https://doi.org/10.1016/j.bmc.2020.115772.

(45) Schmied, W. H.; Elsässer, S. J.; Uttamapinant, C.; Chin, J. W. Efficient Multisite Unnatural Amino Acid Incorporation in Mammalian Cells via Optimized Pyrrolysyl tRNA Synthetase/tRNA Expression and Engineered ERF1. *J. Am. Chem. Soc* **2014**, *136* (44), 15577–15583. https://doi.org/10.1021/ja5069728.

(46) Herring, S.; Ambrogelly, A.; Polycarpo, C. R.; Söll, D. Recognition of Pyrrolysine tRNA by the Desulfitobacterium hafniense Pyrrolysyl-tRNA Synthetase. *Nucleic Acids Res.* **2007**, *35* (4), 1270–1278. https://doi.org/10.1093/nar/gkl1151.

(47) Keeble, A. H.; Turkki, P.; Stokes, S.; Anuar, I. N. A. K.; Rahikainen, R.; Hytönen, V. P.; Howarth, M. Approaching Infinite Affinity through Engineering of Peptide-Protein Interaction. *Proc. Natl. Acad. Sci. U.S.A.* **2019**, *116* (52), 26523–26533. https://doi.org/10.1073/pnas.1909653116.

(48) Zhou, W.; Hankinson, C. P.; Deiters, A. Optical Control of Cellular ATP Levels with a Photocaged Adenylate Kinase. *ChemBioChem* **2020**, *21* (13), 1832–1836. https://doi.org/10.1002/cbic.201900757.

(49) Luo, J.; Uprety, R.; Naro, Y.; Chou, C.; Nguyen, D. P.; Chin, J. W.; Deiters, A. Genetically Encoded Optochemical Probes for Simultaneous Fluorescence Reporting and Light Activation of Protein Function with Two-Photon Excitation. *J. Am. Chem. Soc* **2014**, *136* (44), 15551–15558. https://doi.org/10.1021/ja5055862.

(50) Ramakrishnan, P.; Maclean, M.; MacGregor, S. J.; Anderson, J. G.; Grant, M. H. Cytotoxic Responses to 405 nm Light Exposure in Mammalian and Bacterial Cells:

Involvement of Reactive Oxygen Species. *Toxicol. in Vitro* **2016**, *33*, 54–62. https://doi.org/10.1016/j.tiv.2016.02.011.

(51) Theodosiou, M.; Widmaier, M.; Böttcher, R. T.; Rognoni, E.; Veelders, M.; Bharadwaj, M.; Lambacher, A.; Austen, K.; Müller, D. J.; Zent, R.; Fässler, R. Kindlin-2 Cooperates with Talin to Activate Integrins and Induces Cell Spreading by Directly Binding Paxillin. *eLife* **2016**, *5*, e10130. https://doi.org/10.7554/eLife.10130.

(52) Gasteiger, E.; Hoogland, C.; Gattiker, A.; Duvaud, S.; Wilkins, M. R.; Appel, R. D.; Bairoch, A. Protein Identification and Analysis Tools on the ExPASy Server. In *The Proteomics Protocols Handbook*; Walker, J. M., Ed.; Humana Press Inc., Totowa, NJ, **2005**; pp 571–608.

(53) Rahikainen, R.; Rijal, P.; Tan, T. K.; Wu, H.-J.; Andersson, A.-M. C.; Barrett, J.; Bowden, T.; Draper, S.; Townsend, A. R.; Howarth, M. Overcoming Symmetry Mismatch in Vaccine Nanoassembly via Spontaneous Amidation. *Angew. Chem. Int. Ed.* **2020**, anie.202009663. https://doi.org/10.1002/anie.202009663.

(54) Reichard, E. L.; Chirico, G. G.; Dewey, W. J.; Nassif, N. D.; Bard, K. E.; Millas, N. E.; Kraut, D. A. Substrate Ubiquitination Controls the Unfolding Ability of the Proteasome. *J. Biol. Chem*, **2016**, *291* (35), 18547–18561. https://doi.org/10.1074/jbc.M116.720151.

(55) Ruoslahti, E.; Hayman, E. G.; Pierschbacher, M.; Engvall, E. Fibronectin: Purification, Immunochemical Properties, and Biological Activities. *Meth. Enzymol.* **1982**, *82 Pt A*, 803–831. https://doi.org/10.1016/0076-6879(82)82103-4.

(56) Schindelin, J.; Arganda-Carreras, I.; Frise, E.; Kaynig, V.; Longair, M.; Pietzsch, T.; Preibisch, S.; Rueden, C.; Saalfeld, S.; Schmid, B.; Tinevez, J.-Y.; White, D. J.; Hartenstein, V.; Eliceiri, K.; Tomancak, P.; Cardona, A. Fiji: An Open-Source Platform for Biological-Image Analysis. *Nat. Methods* **2012**, *9* (7), 676–682. https://doi.org/10.1038/nmeth.2019.

(57) Li, L.; Fierer, J. O.; Rapoport, T. A.; Howarth, M. Structural Analysis and Optimization of the Covalent Association between SpyCatcher and a Peptide Tag. *J. Mol. Biol.* **2014**, *426* (2), 309–317. https://doi.org/10.1016/j.jmb.2013.10.021.